Bioethanol separation by a new pass-through distillation process

Janković, Tamara; Straathof, Adrie J.J.; McGregor, Ian R.; Kiss, Anton A.

DOI
10.1016/j.seppur.2024.126292

Publication date
2024

Document Version
Final published version

Published in
Separation and Purification Technology

Citation (APA)
Janković, T., Straathof, A. J. J., McGregor, I. R., & Kiss, A. A. (2024). Bioethanol separation by a new pass-through distillation process. *Separation and Purification Technology*, *336*, Article 126292. https://doi.org/10.1016/j.seppur.2024.126292

Separation and Purification Technology 336 (2024) 126292

Contents lists available at ScienceDirect

Separation and Purification Technology

journal homepage: www.elsevier.com/locate/seppur

Bioethanol separation by a new pass-through distillation process

Tamara Janković [a], Adrie J.J. Straathof [a], Ian R. McGregor [b], Anton A. Kiss [a,*]

[a] *Department of Biotechnology, Delft University of Technology, van der Maasweg 9, Delft 2629 HZ, The Netherlands*
[b] *Drystill Holdings Inc., 3549 Mavis Road, Mississauga, Ontario L5C 1T7, Canada*

ARTICLE INFO

Keywords:
Bioethanol
Distillation
Fluid separation
Process design
Industrial fermentation

ABSTRACT

Distillation is the most used separation technology at industrial-scale, but using distillation in bio-based processes (e.g. fermentation processes to produce bioethanol) is quite challenging when mild temperatures are needed to keep the microbes alive. Vacuum distillation can be used to perform evaporation at low temperatures, but setting a low distillation pressure fixes also the condensation temperature to very low values that may require expensive refrigeration.

Pass-through distillation (PTD) is an emerging hybrid separation technology that effectively combines distillation with absorption in a sorption-assisted distillation process that decouples the evaporation and condensation steps. This is achieved by inserting between the evaporation and condensation steps an absorption-desorption loop that passes through the component to be separated and allows the use of different pressures and types of heating and cooling utilities.

This paper is the first to present the process design and rigorous simulation (implemented in Aspen Plus) of a new pass-through distillation process for bioethanol (~100 ktonne/y plant capacity), proving its effectiveness in concurrent alcohol recovery and fermentation (CARAF). Combining PTD with heat pumps leads to low recovery costs of 0.122 $\$/\mathrm{kg_{EtOH}}$ and energy requirements of only 1.723 $\mathrm{kW_{th}h/kg_{EtOH}}$. Alternatively, combining PTD with multi-effect distillation resulted in 0.131 $\$/\mathrm{kg_{EtOH}}$ recovery costs and 1.834 $\mathrm{kW_{th}h/kg_{EtOH}}$ energy intensity.

1. Introduction

Lower alcohols are important chemicals. For some of them, in particular ethanol, 1-butanol, *iso*-butanol, and *iso*-propanol, fermentative production is feasible or already a reality at large-scale as part of a circular bio-based economy, moving away from fossil carbon sources. A key problem in the field of industrial biotechnology is that bio-alcohols are toxic to cells and thus contribute to fermentation stress and limit the operational range [1]. When the concentration of alcohol increases during fermentation, limits are reached in the productivity, broth titer, yield of alcohol on substrate, and substrate feed concentration [1]. This leads ultimately to high water throughput (diluted aqueous streams), which is associated with large capital expenditure and operating expenses particularly in downstream processing [2]. This end-product inhibition phenomenon, which is the result of solvent toxicity, remains a persistent, unsolved problem for industrial-scale alcoholic fermentations, despite decades of research and development. However, it can be mitigated by continuously removing the product from the broth while fermentation is on-going. This product recovery strategy has been shown in many research studies to be beneficial, but it is not yet widespread in the industrial practice [1,3].

Several industrially promising product recovery strategies have been evaluated at a relevant scale, but all have some drawbacks [1,2]. Such separations fall into four categories (and hybrids thereof): vacuum distillation, gas stripping, membrane pervaporation, and liquid-liquid extraction [2]. One approach for recovery of bio-alcohols is to separate biomass from the fermentation broth prior to product purification. The separated cells can be recycled back to the fermenter. However, regrowing the separated wet cells might be necessary, resulting in lower product yield relative to the substrate. Additionally, some products might easily be separated with the cells which requires additional washing resulting in further dilution that complicates downstream processing. Another option to mitigate the mentioned complications is to use a separation technique that removes the product from the broth while keeping cells viable for recycling with most of the fermentation broth. A crucial requirement in this case is that the recovery process must be conducted at a temperature compatible with the microbes to avoid a negative impact on the cell viability. For example, the optimum

---

[*] Corresponding author.
E-mail address: A.A.Kiss@tudelft.nl (A.A. Kiss).

https://doi.org/10.1016/j.seppur.2024.126292
Received 10 October 2023; Received in revised form 22 December 2023; Accepted 2 January 2024

fermentation temperature for industrial yeast strains in bioethanol fuel production is ~37 °C. Any recovery process operating at a higher temperature will risk cell death, negating any potential benefits [4].

In first-generation fermentation, yeast strains and fermentation management techniques have been improved to such an extent that economically acceptable titers (>10 wt%) and yields (>90 % of the theoretical yield) are possible. For second-generation fermentation, the problem of end-product inhibition is significantly more challenging and a major barrier to commercialization, particularly for advanced biofuels [5]. Microbes are inherently much less tolerant to advanced solvents such as butanol and propanol. Also, the use of lignocellulosic feedstock introduces other complications, as fermentations must tolerate other additional inhibiting compounds (e.g. organic acids, phenolics, and furan derivatives). The need to co-ferment a mixture of C5 and C6 sugars presents a challenge in selecting a suitable microbe. To date, much effort has been put into genetic engineering of an industrially relevant microbial strain that can simultaneously ferment mixed sugars and tolerate inhibitors, while also delivering acceptable titer, productivity, and yield. Unfortunately, genetic engineering to enable metabolism of multiple sugars worsens the tolerance to solvents and other inhibitors. Considerably more attention has been paid to the genetic engineering of strains with special features and tolerances than to recovery technologies. Until an ideal industrial microbe is identified, a stronger focus on the downstream alcohol recovery and separation steps can yield significant commercial progress [6,7].

A practical, low-cost, microbe-compatible separation process is needed to commercialize a concurrent alcohol recovery and fermentation (CARAF) process. Pass-through distillation is a newcomer to the field of industrial separation [8], which may fill this need by addressing some of the practical limitations of distillation in CARAF, and reducing the otherwise high operating temperatures and costs [5].

The process design and simulation play a vital role in the development of sustainable chemical processes, allowing the application of a process systems engineering approach in biotechnology [9,10]. Thus, the main objective of this research is to expand novel implementations of pass-through distillation (PTD) technology. In this respect, the spreading of PTD technology is advanced by presenting the first design of an industrial-scale bioethanol recovery process from dilute fermentation broth. To enhance the performance of PTD, it was coupled with advanced vapor recompression or multi-effect distillation systems. Besides the technical evaluation, an analysis of economic and environmental impact was performed to prove the high competitiveness and effectiveness of this new technology for concurrent alcohol recovery and fermentation. Furthermore, an additional novelty in this work is the development of a reliable property model for a complex system containing an electrolyte (lithium bromide) and two polar solvents (ethanol and water). In addition to continuously removing inhibitory product from the fermentation broth, the proposed recovery processes enable recycle of biomass and most of the water to the fermentation. Consequently, the fermentation may be enhanced by increasing yield, avoiding loss of biomass and reducing water requirements. Thus, the outcome of this work contributes to the advancement of the biotech industry by enabling widespread use of CARAF also to other bio-based processes.

2. Problem statement

In classic distillation, the evaporation and condensation steps are carried out at the same pressure, thus making it difficult to apply to bio-based systems due to the resulting operating temperatures. The selection of pressure in distillation is a key design step, as the pressure will set both the boiling and condensation temperatures, and consequently, the type of heating and cooling utilities needed. Usually, the evaporation temperature should be lower than that of a cheap heating utility (high-pressure steam), and the condensation temperature should be higher than that of a cheap cooling utility (cooling water). But setting a single pressure to satisfy both temperature constraints is not always possible, e.g. in vacuum distillation (used to separate heat-sensitive materials). Vacuum distillation has potential application in the separation of fermentation products, whereby conditions should ensure viability of microorganisms present in the aqueous surrounding. However, the potential challenge is that lowering the operating pressure (to allow evaporation at low temperature) also leads to low condensation temperature that requires expensive refrigeration utilities instead of cheaper cooling water. This issue can be solved conveniently by pass-through distillation, which inserts an absorption-desorption loop between the evaporation and condensation steps such that it decouples them in terms of pressure [10]. The evaporator pressure can now be sufficiently low to allow boiling at temperatures that do not exceed the defined upper limit, while the condenser pressure is sufficiently high to allow condensation at temperatures suitable for using conventional utilities.

3. Pass-through distillation technology

3.1. Working principle

The working principle of pass-through distillation (a novel sorption-assisted fluid separation process) is illustrated in Fig. 1. Evaporation and condensation steps can take place at different pressures by using an absorption-desorption loop that decouples them. Decoupling allows the evaporator to operate at very low pressure (and thus low temperature) while the condenser operates at higher pressure (low-cost cooling). A PTD process involves three main pieces of equipment: an evaporator, a gas/vapor absorber, and a regenerator for the absorption fluid (shown schematically in Fig. 2). A liquid feed stream is fed to an evaporator vessel, where a part of it is turned to vapor that leaves the evaporator through a port near its top, while the unevaporated portion leaves the vessel as a bottom stream. The vapor from the evaporator is then drawn through an absorber vessel where it contacts an absorbent fluid. The absorption fluid must have a very low vapor pressure and a high affinity for the main chemical constituents in the vapor generated by the evaporator. Solutions of highly hygroscopic and water-soluble salts are good non-volatile candidates for PTD in aqueous service, e.g. lithium bromide (LiBr), lithium chloride (LiCl), and calcium chloride ($CaCl_2$). LiBr brine is used in the absorption chiller industry and dehumidification equipment, being the least corrosive of the salts mentioned [11,12].

When water or polar compounds (e.g., alcohols) must be removed, a concentrated LiBr solution can be used as hygroscopic working/absorbent fluid. This brine absorbs the vapor coming from the evaporator (where the saturated feed is evaporated at low pressure) and leaves the vessel at the bottom, as part of a diluted brine solution. The diluted working fluid is pumped to the desorber/regenerator (a conventional still), where the passed-through components are evaporated at a higher pressure (using external heat) and then condensed using cooling water. Even though in the PTD process the same components are evaporated twice, there are possibilities for significant energy savings. Firstly, the heat released during absorption can be reused for the evaporation step. These operations can be fully integrated into a single unit (as shown in Fig. 2), known as a stripping-absorption module (SAM) [13] – described in more detail in a later section. In this equipment unit, heat pipes are used to transfer in-situ the heat released by absorption to the evaporation section of the unit. In the SAM, the evaporator and absorber work essentially at the same absolute pressure. Notably, PTD does not necessarily require a SAM in order to work, but this is one of the best solutions for effective heat transfer from the absorption to the evaporation step. Secondly, there are different possibilities for enhancing the desorption part of the PTD. This original research analyses in more details the energy savings that can be obtained by using advanced heat pumping systems (vapor recompression), or multi-effect distillation (MED) in this step.

The main advantages of PTD are the following: applicability to heat-sensitive materials, avoidance of expensive refrigeration utilities, smaller equipment size compared to vacuum distillation technologies

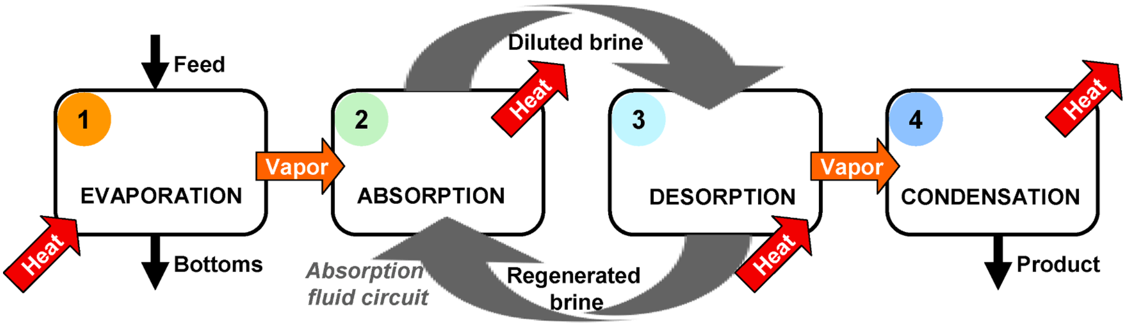

Fig. 1. Working principle of pass-through distillation, based on an open loop absorption/desorption cycle inserted in-between evaporation and condensation.

and highly competitive energy requirements [8].

3.2. Pilot plant development

Drystill has invented and patented a stripping absorption module (SAM) as an innovative heat and mass exchange device that can enhance the overall pass-through distillation (PTD) process [13]. Furthermore, proprietary SAMs were built and tested at bench- and pilot-scale to prove the effectiveness of this new technology. Lithium bromide and lithium chloride solutions have both been successfully used as absorbent fluids [5]. The constructed pilot plant (Fig. 3) features a SAM with 100 copper heat pipes (25 mm in diameter by 55 cm in length) that could boil water at a temperature as low as 20 °C and a rate of up to 50 kg/h. Additionally, a single-effect regenerator was included to provide reusing of brine and maintain continuous operation practically indefinitely [5]. Both watery and high-solids aqueous slurries have been successfully tested in this pilot project.

4. Results and discussion

This section describes the main results related to the design and simulation of a PTD process used for concurrent alcohol recovery and fermentation in bioethanol production. Since this novel technology implies the usage of an electrolyte solution to absorb ethanol, with some water, from the fermentation broth, a reliable property model had to be developed first to accurately account for all interactions in this complex system. A bioethanol purification process using PTD was designed to obtain a high-purity final product (99.8 wt%), with a production capacity of 100 ktonne/y. Heat integration and heat pumping options were proposed. Finally, a complete analysis of process performance, both in terms of economic and sustainability indicators, was conducted to prove the competitiveness and effectiveness of the newly proposed design.

4.1. Property model

Modeling a PTD process is challenging in terms of physical properties due to the presence of the absorbent fluid (LiBr – water). There are a number of commercial platforms available which are able to model such systems, e.g. Engineering Equation Solver (EES), Absorption Simulator (ABSIM) or Aspen Plus [14]. While there is previous work on binary systems ethanol – water (including CO_2 and other organic impurities) [15,16], LiBr – water [17], and LiBr – ethanol [18], this work is the first to bring together all components in a unique process design. Modeling the ternary system LiBr – ethanol – water is complex since the interactions between the electrolyte and the two solvents need to be considered. Additionally, a proper thermodynamic model must account for the interactions between two polar solvents. Accurate modeling of relations between these components is a crucial aspect in further development of reliable process simulations.

The electrolyte-NRTL (Pitzer-Debye Hückel) model combined with the Redlich-Kwong equation of state, known as ElecNRTL-RK, was used in Aspen Plus as the most suitable option [19]. It describes the Gibbs excess energy using local compositions and is applied to a completely dissociated electrolyte. The model works well over extensive concentration and temperature ranges making it extremely useful in process modeling [7]. The ElecNRTL-RK model characterizes the behavior of ternary systems by using binary interactions [20]. Therefore, regressions based on experimental data for binary systems [15,17,18] were used in Aspen Plus to determine the binary interaction parameters (BIPs) that properly describe the complex ternary system. However, the deviation of the obtained property model from the available literature data for the system LiBr – ethanol was significant (over 40 %).

To solve this problem, a published method for predicting salting effects in ternary salt – alcohol – water systems [21] was used to estimate the equilibrium data for the LiBr – ethanol – water mixture. This methodology implies using Tan's modification of the Wilson model to account for both solvent – solvent and solvent – electrolyte interactions in the complex ternary system. Solvent – solvent interaction parameters and vapor pressure data for electrolyte – solvent systems are used to predict equilibrium data for the ternary system [21]. The estimation of the data for the system LiBr – ethanol – water was performed in MATLAB. The data predicted using this method were included in the BIPs regression in Aspen Plus for the system LiBr – ethanol, with a lower weight factor compared to the experimental data. Consequently, the deviation between regressed data and literature data for system LiBr – ethanol decreased significantly (to about 3.8 %). The comparison of the property model with experimental data is provided in the Supplementary Information file.

Additionally, since experimental data for system LiBr – ethanol are available for up to 23 wt% LiBr, recommendations from the literature [22] were used to estimate the equilibrium data for higher LiBr concentrations. The proposed relation describes the dependency of the vapor pressure of an electrolyte – solvent system on the temperature, ionic strength, molecular weight, electrolyte and solvent parameters. As temperature, ionic strength and molecular weights are fixed for a certain system, the electrolyte and solvent parameters are variable. Initially, the vapor pressures calculated using literature parameters for LiBr – ethanol mixture were compared with the available experimental data [18]. Since the total deviation was about 9.7 %, data regression was performed in MATLAB to update the values of the electrolyte and solvent parameters. Literature data for these parameters were used as initial values, while the mean relative error was used as objective function to be minimized. The electrolyte and solvent parameters determined in this way resulted in only about 0.8 % deviation from the available literature data for the LiBr – ethanol system. Changes in values of parameters used for vapor pressure calculation and the comparison with experimental data are summarized in the Supplementary Information file. The parameters obtained were used to estimate data for higher concentrations of LiBr in the LiBr – ethanol system. These data were included in BIPs regression in Aspen Plus, also with a lower weight factor compared to the experimental data [18]. The deviation of regressed data from the literature data [18] for LiBr concentrations higher than 15 wt% was

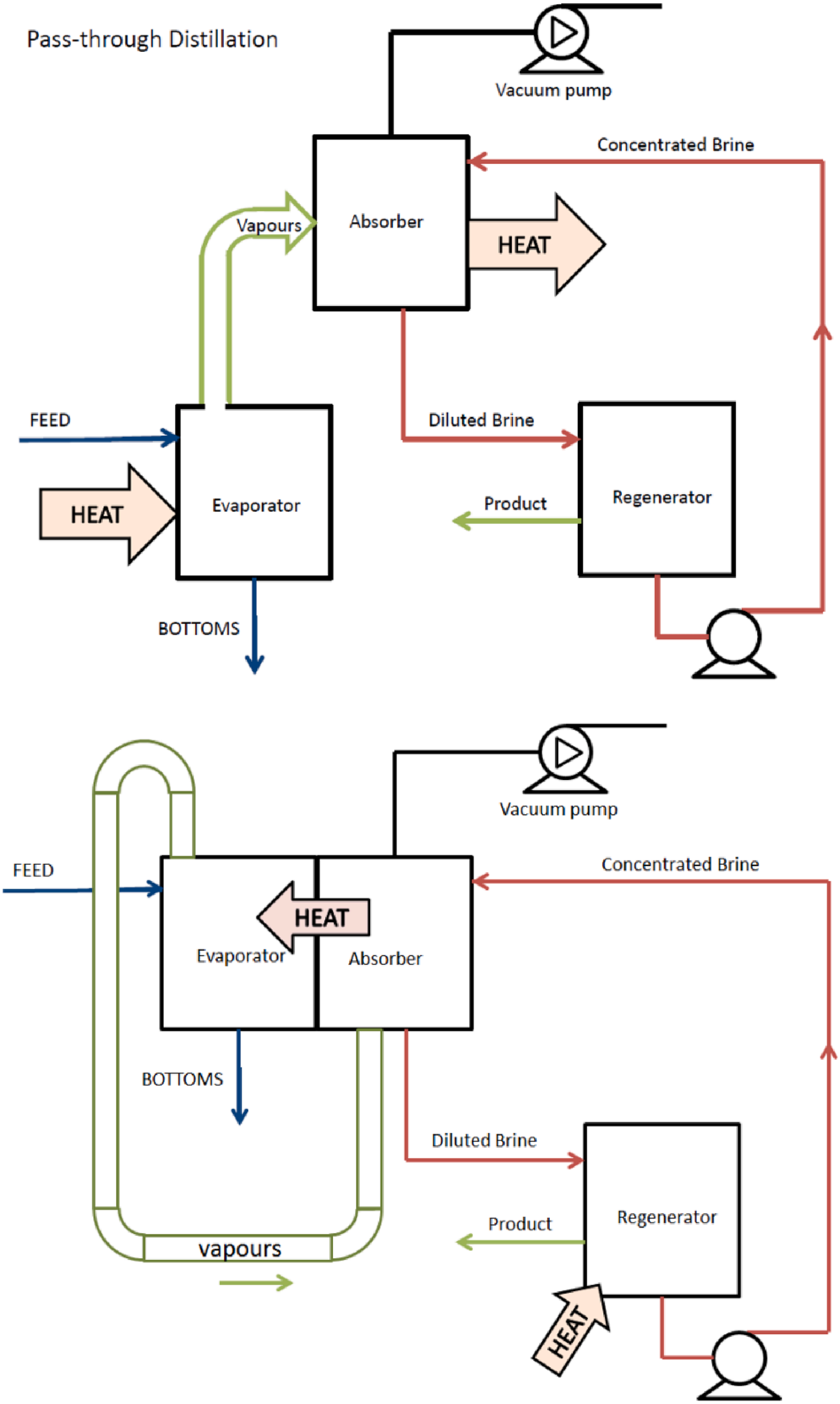

Fig. 2. Schematics of a pass-through distillation process: without and with thermally integrated evaporation and gas absorption (TIEGA).

Fig. 3. Pass-through distillation pilot-scale unit in operation at Fielding Chemical Technologies, where the stripping-absorption module built by Drystill plays a key role [8].

reduced from about 8.0 % to 5.9 %, whereby the total deviation (along the whole concentration range) was reduced to less than 3.2 %.

The values of BIPs obtained by performing the parameter regression in Aspen Plus are summarized in Table 1. The adequacy of the proposed property model was proven by comparing the predicted values with experimental data available for all binary systems [15,17,18]. This comparison is presented in Fig. 4. The deviation of the T-xy diagram for the system ethanol – water generated with the developed property model vs experimental data [15] is only 0.5 %. The predicted vapor pressure for the system LiBr – water differs from literature data [17] by 6.5 %. Lastly, the deviation of the predicted vapor pressures for the system LiBr – ethanol from the values reported in the literature [18] is less than 3.2 %.

An additional validation of the proposed property model was performed by comparing the predicted data for the ternary system LiBr – ethanol – water against experimental data for similar systems using $CaCl_2$ or $ZnCl_2$ as salts [23]. As $CaCl_2$, $ZnCl_2$ and LiBr are all highly hygroscopic and water soluble salts [24], a similar behavior can be expected when dissolved in ethanol – water solvent mixtures. The results of the comparison for isobaric systems with different salt concentrations are presented in Fig. 5. Very similar trends can be observed, which confirms that the property model for the system LiBr – ethanol – water is reliable.

Lastly, since the effective ethanol recovery from the fermentation broth is the main goal of this study, the dependency of the ethanol mass fraction in the vapor phase from the ethanol mass fraction in the liquid phase in the ternary system LiBr – ethanol – water is presented in Fig. 6.

Table 1
ElecNRTL-RK binary interaction parameters for water (i) – lithium bromide (j) and ethanol (i) – lithium bromide (j).

Parameter	Molecule or Electrolyte		Molecule or Electrolyte		Value
$c_{i,j}$	H_2O		Li^+	Br^-	49.1146
$c_{j,i}$	Li^+	Br^-	H_2O		–23.7669
$d_{i,j}$	H_2O		Li^+	Br^-	2201.39
$d_{j,i}$	Li^+	Br^-	H_2O		−915.851
$e_{i,j}$	H_2O		Li^+	Br^-	−70.3447
$e_{j,i}$	Li^+	Br^-	H_2O		31.2823
$\alpha_{i,j}$	H_2O		Li^+	Br^-	0.0335707
$c_{i,j}$	Ethanol		Li^+	Br^-	83.1575
$c_{j,i}$	Li^+	Br^-	Ethanol		−47.6692
$d_{i,j}$	Ethanol		Li^+	Br^-	−2447.64
$d_{j,i}$	Li^+	Br^-	Ethanol		2822.35
$e_{i,j}$	Ethanol		Li^+	Br^-	−905.818
$e_{j,i}$	Li^+	Br^-	Ethanol		486.525
$\alpha_{i,j}$	Ethanol		Li^+	Br^-	0.0199508

4.2. *Process design and simulation*

Using the reliable property model developed, the recovery of bioethanol from a fermentation broth by PTD was designed. Rigorous process simulations were developed in Aspen Plus.

4.2.1. *Setting of initial conditions*

The feed to the PTD process is the fermentation broth containing ethanol, water, carbon dioxide (CO_2), as well as non-volatile microorganisms and inert components (which can be neglected in the simulation, as they are removed in the first step without evaporation). The feedstock for this process was considered to have an ethanol concentration of 5 wt%, being on the lower side of typical broth concentrations after fermentation [2,25]. The feed flowrate was chosen such that ~100 ktonne/y of ethanol can be recovered. Furthermore, the broth was considered at 37 °C and 1 bar [4]. As CO_2 is a key metabolic product of microorganisms in the fermenter, it is present in the fermentation broth sent to downstream processing. The CO_2 concentration in this stream (0.1 wt%) is equal to its solubility in water at 37 °C and 1 bar [26].

Due to the presence of CO_2 in the feed stream, the first step in the ethanol recovery is the removal of some of the CO_2 using a degasser unit. The operating pressure for this step (0.065 bar) was chosen such that over 50 % of the initially present CO_2 is removed. However, pressure reduction causes vaporization of some ethanol and water from the feed stream. As much as 4.3 % of initially present ethanol is removed together with CO_2 and some water, as carbon dioxide also serves the purpose of removing ethanol from a liquid solution [27]. That ethanol is recovered later (see section 4.2.4).

4.2.2. *Evaporation and absorption parts of PTD*

The evaporation and absorption parts of PTD can be coupled and performed in one process unit. The stripping absorption module (SAM) is a specific piece of equipment developed by Drystill [13], which uses the heat of absorption to vaporize the feed. SAM is basically an evaporator and gas absorber combined in a single low pressure vessel, with heat pipes passing through the bulkhead that separates them. Heat pipes conduct heat from the hot absorber to the relatively cooler evaporator. The evaporator generates vapors that are ducted into the gas absorber and absorbed into a stream of absorbent fluid. Under the right conditions, the heat demanded by the evaporator is exactly matched to the heat supply from the absorber, and the SAM will operate with no externally applied heating or cooling. So roughly the same quantity of heat is involved by each process – the latent heat of evaporation [5]. This piece of equipment is not available off-the-shelf in the process simulator

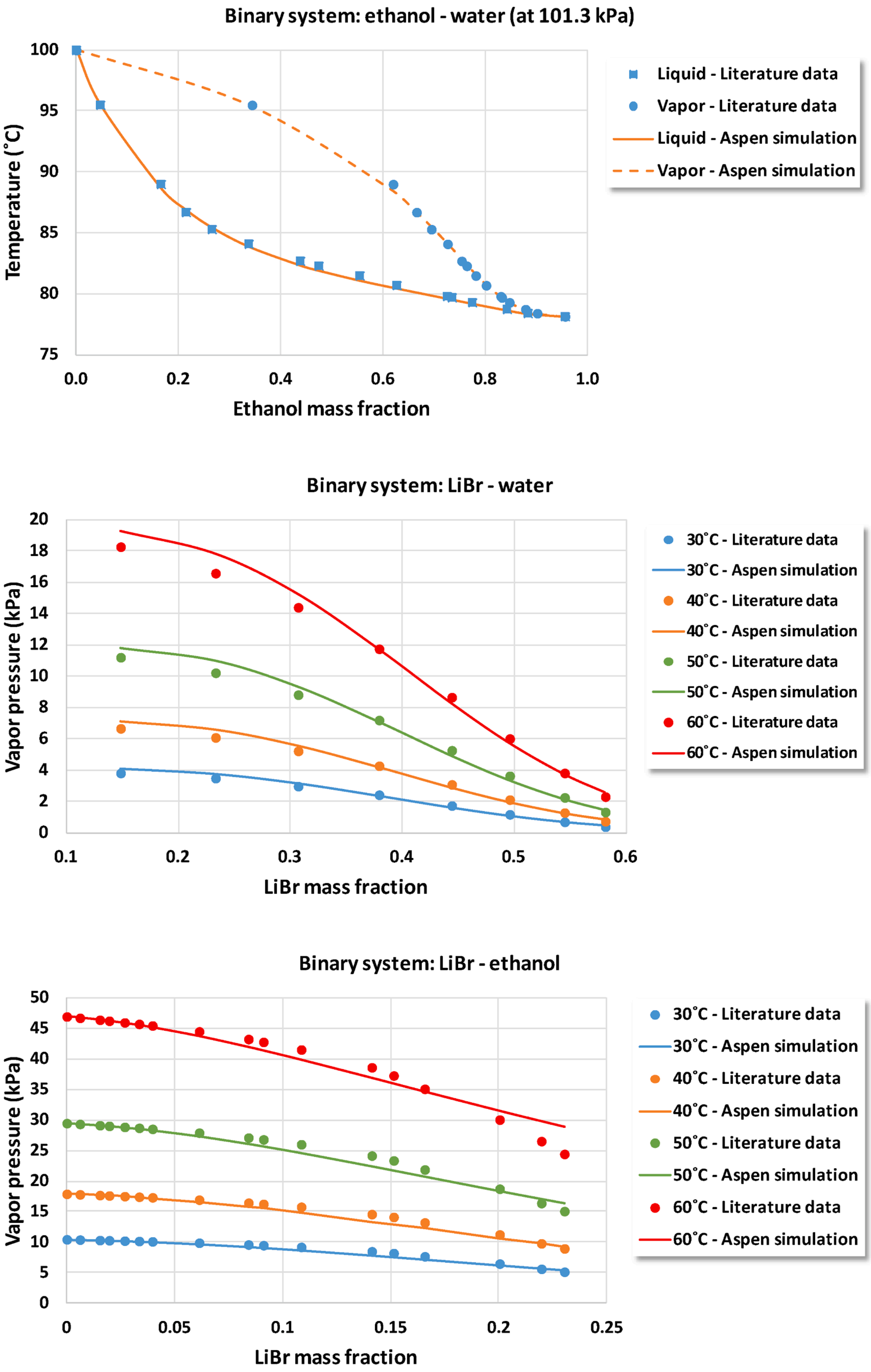

Fig. 4. Comparison between the results predicted by the developed Aspen Plus property model (ElecNRTL-RK) and literature data [15,17,18].

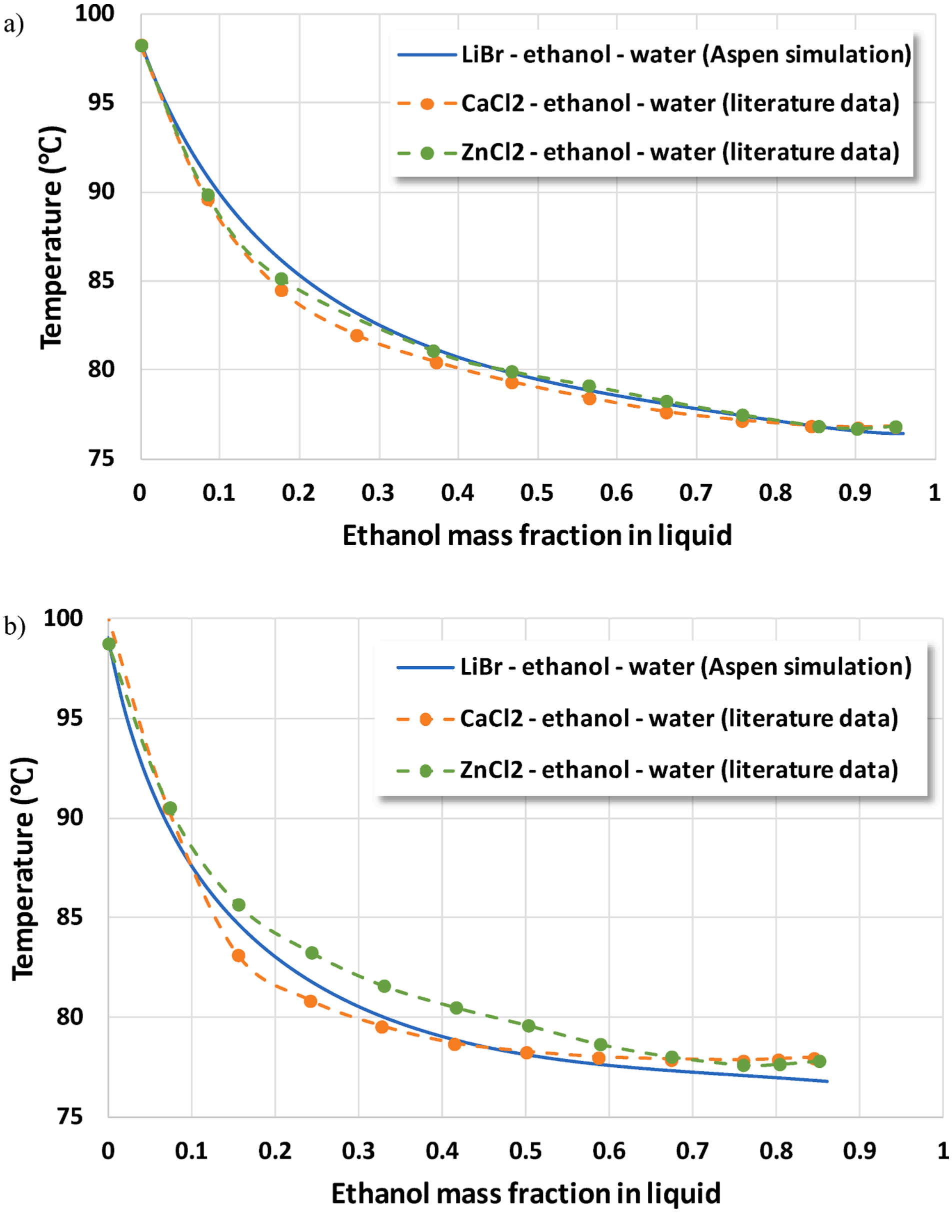

Fig. 5. Comparison between the results predicted by proposed Aspen Plus property model for system LiBr – ethanol – water with literature data [23] for systems $CaCl_2$ – ethanol – water and $ZnCl_2$ – ethanol – water at pressure of 94.5 kPa: a) 5 wt% of salt in liquid, b) 15 wt% of salt in liquid.

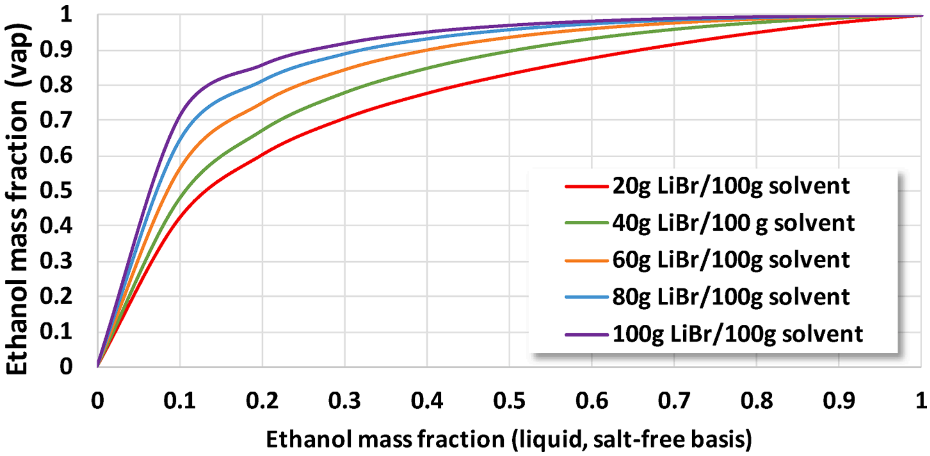

Fig. 6. Predicted ternary data by the Aspen Plus property model (ElecNRTL-RK) for the ternary system LiBr – ethanol – water (at 50 ℃).

(Aspen Plus) so it has to be described via an equivalent combination of unit operations – as shown in Fig. 7. The SAM is operated under reduced pressure so that ethanol and water vapor can be produced from the fermentation broth without the temperature exceeding the optimum fermentation temperature. A temperature in the region of 37 °C (as the upper limit) needs to be maintained for the optimum ethanol production rate [4]. Operating below this temperature also maintains a degree of safety, such that in the case of a deviation from normal operation, a temperature rise will not cause damage to the used microorganisms.

Vaporization taking place in the SAM aims to maximize the ethanol concentration in the vapor phase product that is sent to the absorber unit. The remaining liquid from the evaporation step contains most of the water and microorganisms. This stream can be recycled to the fermenter to avoid biomass loss and allow fermentation to be performed in a closed loop [28]. This flash step is achieved by heat transfer from the hotter absorbed fluid. The operating pressure of the SAM was determined such that the addition of heat to the feed broth causes the evaporation of the material. Fig. 8 can be used to select an appropriate operating pressure in the SAM. As broth temperature after the degassing step is reduced to about 34 °C, the SAM operating pressure was varied while keeping the temperature constant. As the total vaporization happens at 0.054 bar, this pressure value was chosen for operation.

The flow rate of LiBr/water solution relative to the vapor feed is another operating parameter that has a key effect on the process design. A feed temperature of the lithium bromide solution of 50 °C, and a concentration of ~50 wt% were considered as suggested in literature [29]. Absorption is exothermic and releases heat that is used to evaporate ethanol and water vapor from the fermentation broth. The heat exchange that occurs in the SAM is not achieved by a heat exchanger, but rather by heat pipes between the two chambers. Heat pipes are known for their ability to transfer substantial quantities of heat with a nominal temperature difference (5 K) driving force [30]. The flowrate of LiBr brine was varied until the diluted brine stream (after the absorption step) was able to provide the heat required for the evaporation step. This leads to a minimum absorbent to feed ratio of 1.4 on a mass basis. Fig. 8 shows that bringing concentrated LiBr brine into contact with ethanol and water vapors leads to a jump in temperature, which reflects the release of energy during the absorption process. However, the temperature at the outlet from the absorber increases gradually with increasing absorbent flow. It has been already proven that the inlet brine flowrate has a small effect on the temperature difference obtained during the absorption process [31]. The required flowrate of concentrated LiBr brine was determined by the minimum heat capacity of the diluted brine needed to provide heat for the evaporation step.

In the initial design of the SAM unit, to obtain ~19 wt% of ethanol in the vapor after the evaporator unit, as much as 35 % of ethanol from the

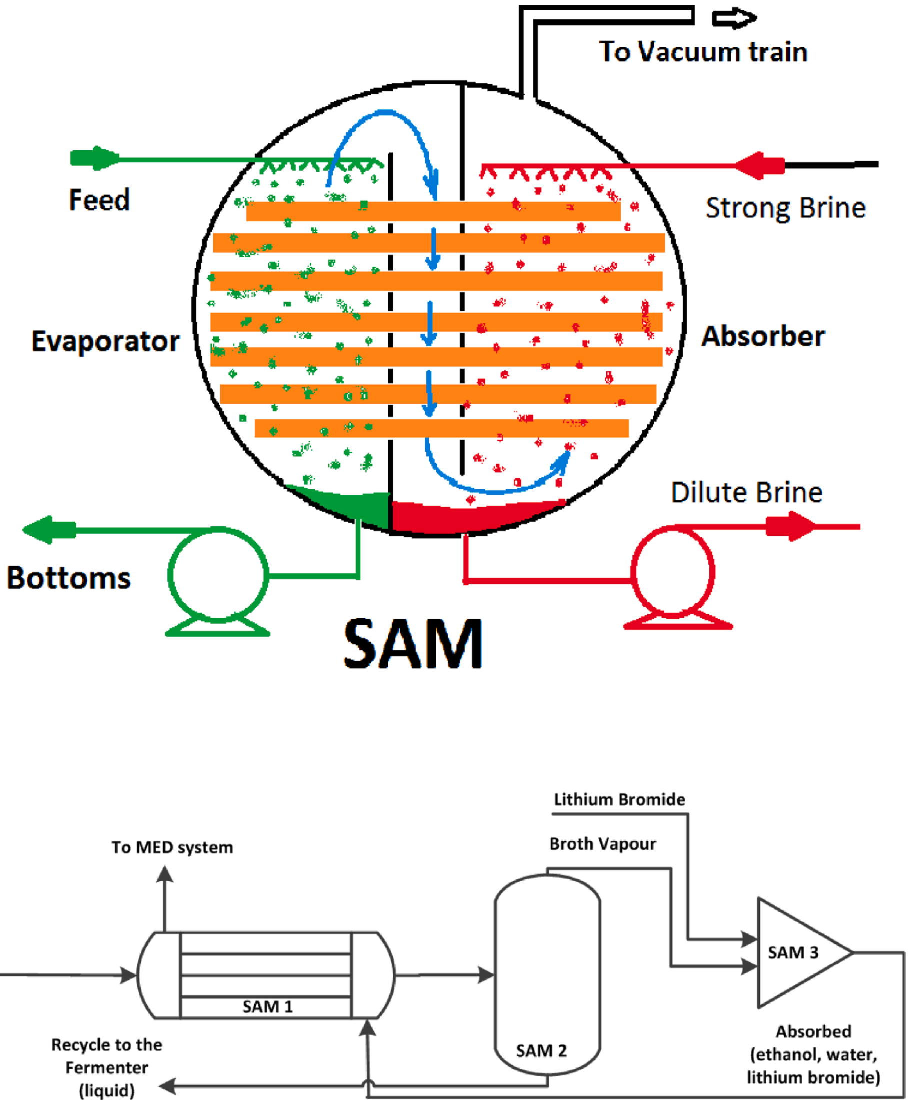

Fig. 7. Stripping-absorption module (SAM) working principle and the corresponding equivalent of conventional units (usable in Aspen Plus simulations).

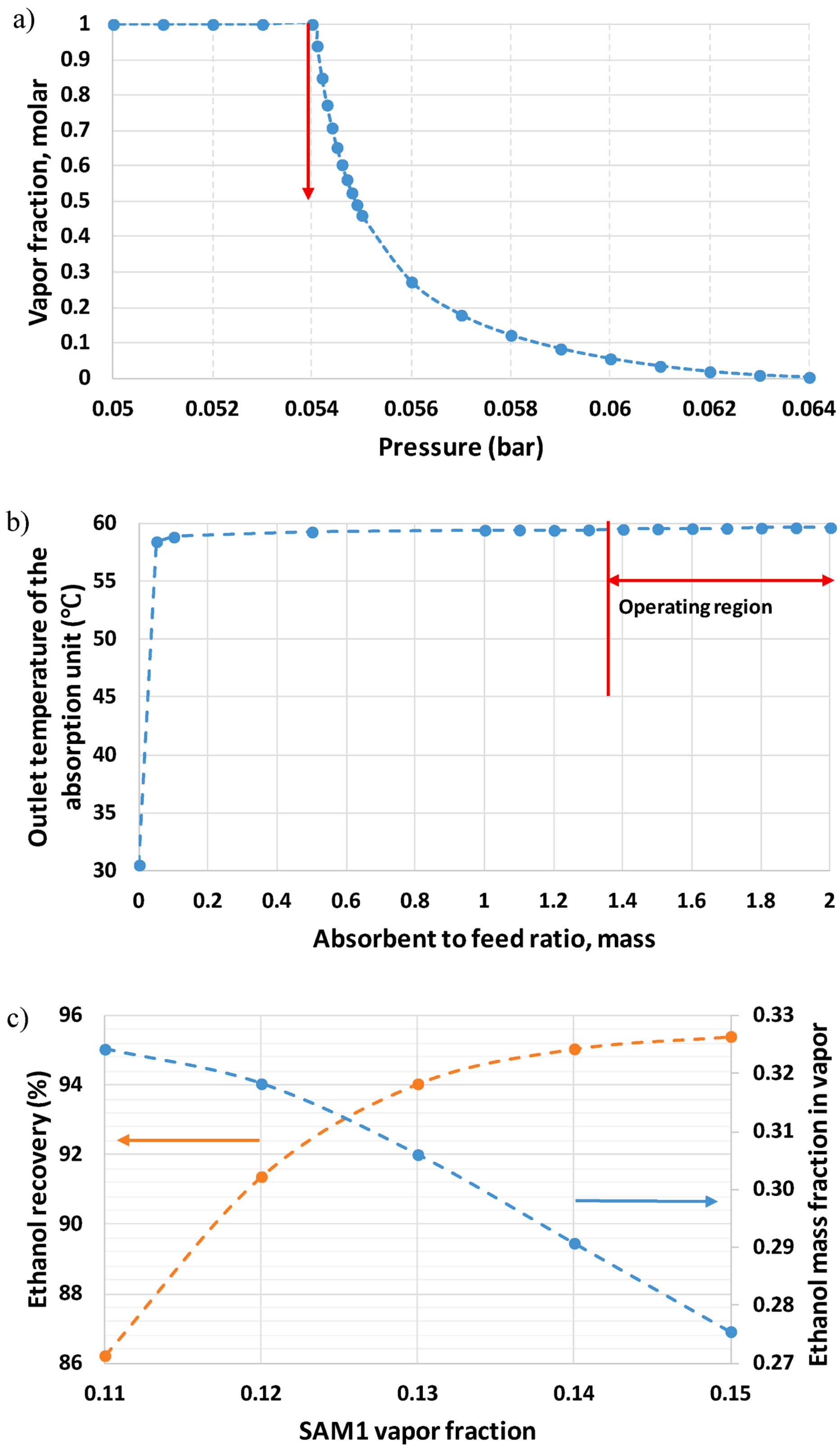

Fig. 8. Design parameters of the SAM unit: a) vapor fraction of the fermentation broth at varying pressures at 34 °C (chosen value is 0.054 bar), b) dependence of the outlet temperature of the SAM on the absorbent to feed ratio (chosen value is 1.4), c) dependence of the ethanol recovery and concentration in vapor phase on vapor fraction of the SAM evaporator part (chosen value is 0.125).

feed stream remains in the broth that is recycled to the fermenter. In addition to not fully recovering the main product, recycling this stream with ~2 wt% of ethanol to the fermenter is not favorable due to the inhibitory effects ethanol has on microorganisms [32]. Higher concentrations of ethanol in the separated vapor would lead to even less recovery, while lower concentrations are not convenient for further downstream processing. To increase ethanol concentration in the vapor sent to the absorber unit, and to minimize both the loss of ethanol and its concentration in the recycle stream, a stripping column was added prior to the SAM unit. Ethanol from the liquid product of the degasser unit is stripped with vapor formed in the evaporator unit of SAM. The liquid product from this stripping column is sent to the evaporation part of SAM, while the vapor product, rich in ethanol, is sent to the absorption part of SAM (Fig. 9 and Fig. 11). This additional column brings several benefits: the vapor sent to the absorption part of SAM contains ~32 wt% of ethanol, whereby only ~3 % of ethanol from the feed stream remains in the recycle stream that has now less than 0.2 wt% ethanol. Therefore, ethanol loss is reduced by about 91 %, while the stream being recycled to the fermenter contains amounts of ethanol that cause negligible inhibition of the microbes. The added stripping column also operates under reduced pressure, thus structured packing type Sulzer Mellapak 250 was selected as internals, with a pressure drop of 0.225 mbar per theoretical stage [33].

The performance of the evaporator was optimized by varying vapor fraction (defined as an operating parameter for the heat exchanger in Aspen Plus representation of the SAM unit) and analyzing effects on the ethanol recovery and concentration in the vapor stream being sent to the absorber part of SAM (see Fig. 8). Higher ethanol concentrations in the vapor, which is more favorable for further purification process, result in lower recovery since more ethanol remains in the stream being recycled to the fermenter. A vapor fraction of 0.125 was chosen for the evaporation part of the SAM, since at this value the ethanol concentration in the separated vapor is higher than 30 wt%, while the recovery is higher than 92 % (value before recovering ethanol separated with CO_2, see section 4.2.4).

4.2.3. *Desorption and condensation parts of PTD*

To recycle the absorbent fluid in a continuous circuit, the diluted brine (coming from the SAM) must be regenerated to its original concentrated state, by desorption. This process involves evaporating all components that have been absorbed during the transit through the SAM absorber chamber. Separated ethanol and water vapor is further condensed and sent to additional purification. The desorber unit can operate at higher pressures and higher temperatures since the brine contains no temperature-sensitive substances (those being removed already as bottoms of the SAM). Thus, following the desorption step, condensation is also performed at higher temperatures which allows the use of cooling water rather than expensive refrigeration.

While the SAM ensures an effective heat recovery from the absorption to the evaporation step, the desorption step still requires external heating. Therefore, different process integration opportunities can be considered to obtain maximal energy savings. Two alternatives for enhancing the desorption and condensation parts of PTD process were analyzed in this original study: usage of heat pumping systems and implementation of multi-effect distillation (MED). As the temperature difference between the vapor phase and the concentrated brine is negligible, heat pumping can be effectively used to reduce the energy requirements. In this system, the formed vapor can be compressed (leading to a temperature increase), and used to evaporate the diluted brine. Thus, the electrical energy needed for compression replaces the much higher thermal energy required initially. Alternatively, the high heating requirements of the desorption step can be significantly reduced by applying MED. This heat integration method implies splitting the diluted brine stream and reusing heat supplied to the high pressure part of this brine to heat up other parts of the diluted brine [34].

Configuration 1: Heat pump assisted desorption and condensation

The first configuration is based on heat pump (vapor recompression) assisted desorption of the PTD, noted here as PTD-VRC (see Fig. 9, further discussed afterwards). The diluted brine from the SAM unit should be pumped to an appropriate pressure for the desorption and condensation steps that follow. As evaporating ethanol and water from the diluted brine is very energy demanding (~25 MW of heating duty for this plant capacity), advanced energy-saving techniques should be implemented. The desorbed vapor can be compressed and used to evaporate part of the diluted brine in the desorber unit. This heat pumping design significantly reduces the external heating for the desorption step. The performance of PTD process was optimized by determining the desorption operating pressure that minimizes the total energy requirements (considering both thermal and electrical energy) for this part of the bioethanol recovery process. Besides minimum temperature difference to ensure efficient heat exchange, an additional limitation of this optimization process is that the resulting temperature for the condensation part should allow the use of cooling water as a cheap utility. As the specific energy requirements (per kg ethanol) for the PTD process are the lowest at 0.2 bar (Fig. 10), this value was chosen as the optimal operating pressure for the desorption and condensation parts. Expensive refrigeration is avoided at this operating pressure since a condensation temperature of ~72 °C is suitable for using cooling water. After evaporating ethanol and some water, the regenerated LiBr brine can be recycled and reused in the SAM unit [8].

A potential limitation for applying this heat pump assisted design for the desorption part is the relatively high temperature of the compressed vapor (about 254 °C) that is needed to provide sufficient heat in the desorber unit. However, the temperature of the compressed vapor should not present a constraint as specific industrial compressors have been designed for much higher outlet temperatures – such as centrifugal compressors offered by MAN Energy Solutions [35]. Furthermore, the outlet temperature from the compressor is reduced after applying heat integration (more details in section 4.2.6).

Configuration 2: Multi-Effect Distillation (MED)

An alternative option is replacing the desorber unit in PTD with multi-effect distillation (MED) to enhance the desorption part, a combination noted here as PTD-MED (see Fig. 11, further discussed afterwards). In this case, the brine may be regenerated using less than half the energy that is originally delivered by the heat pipes into the SAM evaporator.

In this work, three MED stages were chosen (as typical in industry to balance the equipment cost vs. energy savings) such that the feed stream (the diluted brine after the SAM unit) is split into high pressure (HP), medium pressure (MP) and low pressure (LP) streams. Other configurations are also possible. However, adding more stages in the MED results in higher capital costs due to additional equipment units. Furthermore, with increasing the number of MED stages, the temperature within the first distillation stage rises, which might increase operating costs and cause thermally induced fouling of the MED installations [8].

One of the key advantages of PTD is the decoupling of the evaporation and condensation processes. The inserted absorption step allows the liquid stream to have its pressure altered more easily, thus allowing MED to be used to desorb ethanol and water resulting in energy savings. Multiple flash vessels are used at different pressure levels to provide heat recovery from the hotter, higher-pressure streams to the cooler, lower-pressure ones. For a given split ratio, there is a minimum pressure difference required between the MED pressure levels to give a temperature gradient sufficiently large such that efficient heat transfer is possible. For a sufficient temperature difference between the hot and cold streams to produce the specified vapor fraction, there is a minimum operation pressure for the MED stages. The higher-pressure levels can be operated at any pressure above this (not necessarily optimally) and deliver the required heating effect. This means that a direct link can be made between the split ratio of the streams that enter the MED process and the

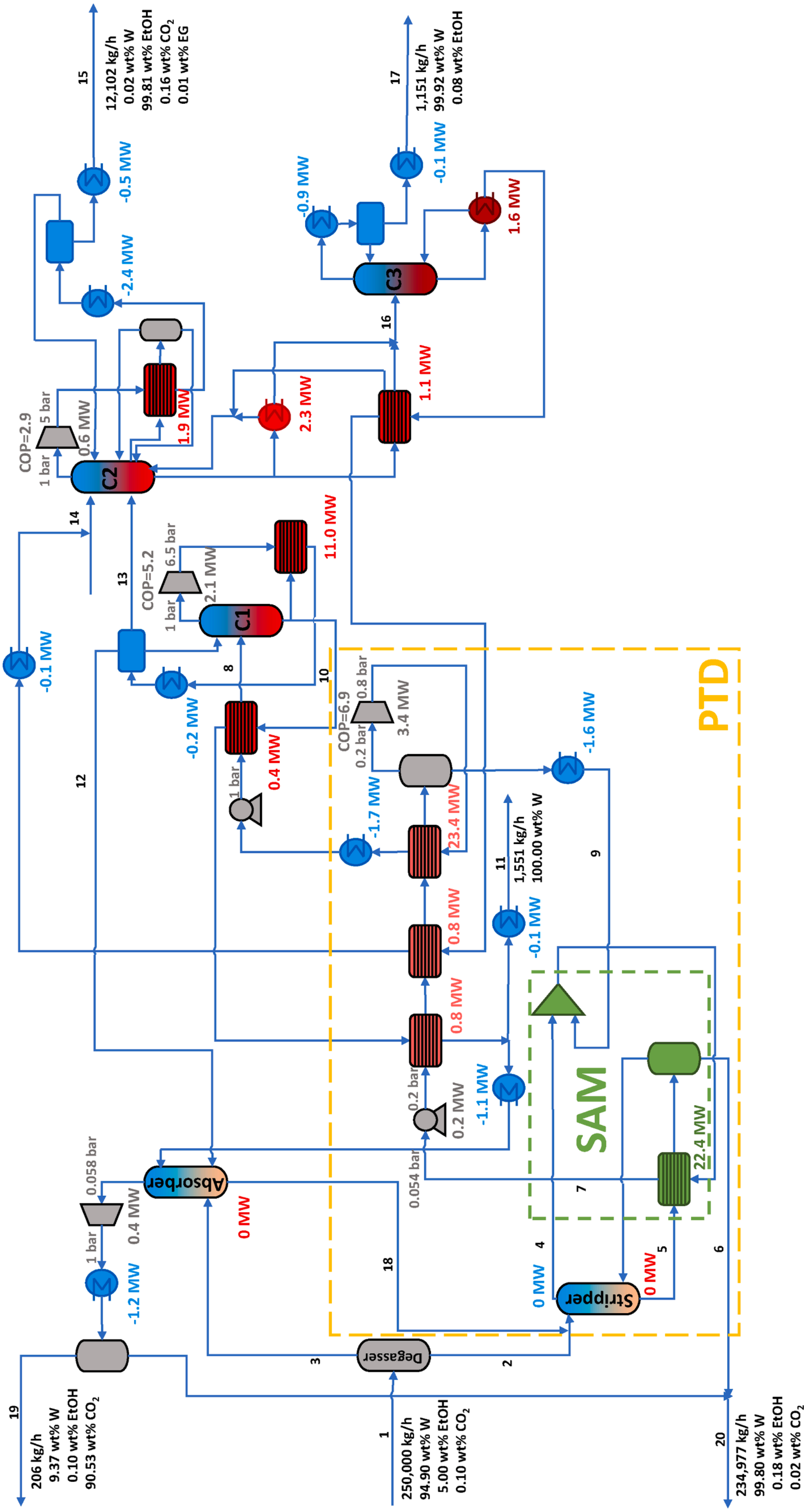

Fig. 9. Flowsheet of the bioethanol recovery from the fermentation broth by process configuration 1 (PTD-VRC) – heating duties (red), cooling duties (blue), compressor/pump duties (grey), water (W), ethanol (EtOH), ethylene glycol (EG); condition and composition of numbered process streams are presented in Table 4.

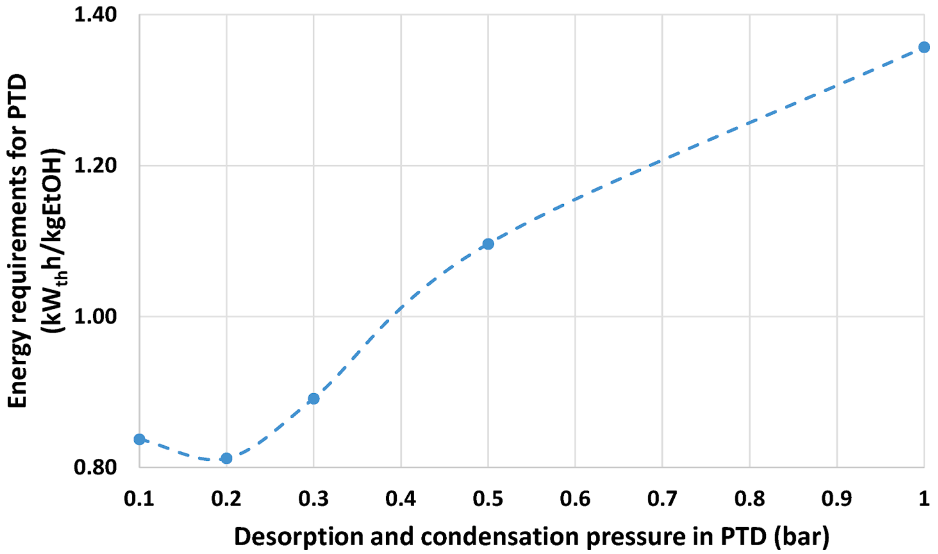

Fig. 10. Influence of operating pressure for desorption and condensation parts of PTD process on energy requirements.

minimum operating pressures. The minimum operating pressure for each stage, which does not lead to a temperature crossover in heat exchangers, is the dependent variable.

The optimization of the PTD process with MED implied identifying the split ratio that results in minimal total energy requirements for this part of the bioethanol recovery process. Split ratios in the vicinity of a value of 1 were explored. It should be noted that a split ratio of 1.2, for example, means that the ratio between the flowrates of the HP and MP streams and the MP and LP streams is 1.2. The split ratio was changed in the Aspen Plus simulation and the minimum pressure was established by manually adjusting the pressure in the MP and HP streams until there was no temperature crossover detected. The pressure of the LP stream (0.09 bar) was defined in a way that allows later condensation with cooling water. The MP and HP streams need to take a pressure that gives the product streams of the flash unit temperatures that allow the necessary heat transfer to take place.

Fig. 12 gives a visual representation of how the required pressure of each stream changes with differing split ratios. As the split ratio increases, such that more flow is sent to the higher-pressure streams, the pressure needed in the HP and MP levels is reduced, whereby these changes are more noticeable for the HP stream. A higher flow rate in the HP stream for example gives it a higher heat capacity flow rate, reducing the change in temperature required by that material to deliver a certain amount of heating. A lower inlet temperature of the hot stream in the heat exchanger is therefore required to meet the cold stream outlet specification and thus a lower pressure is needed. For split ratios above roughly 1.05, this pressure change is rather gradual. Below this, however, a vast increase in pressure is required as the hot vapor stream is cooled so much that it completely condenses and becomes a liquid. At this point, its temperature falls drastically until it is the same as for the cold stream, and a temperature cross is detected. Below a split ratio of 0.95, the pressure required rises so significantly that it would be completely impractical and hence is not included in this study. Fig. 12 suggests that a split ratio of above 1.05 is sensible due to the minimization of the operating pressure required. A split ratio above this value will result in a further reduction in operating pressure and in a decrease in temperature of hot utility required to achieve vaporization in the HP stream. Yet, this advantage comes at a decreasing rate (shown by the reducing gradient in Fig. 12), at the expense of a higher flow rate to be heated by the utility, hence increasing process energy requirements. Therefore, analysis of energy requirements for the MED part of the process depending on defined split ratio was performed and results are also presented in Fig. 12. Both thermal and electrical energy requirements were included in this analysis (as described in a later section). With a defined split ratio of 1.05 total energy requirements are the lowest, while the required pressure for the HP stream is reasonable (~2 bar). Therefore, this value was chosen as the optimal one for splitting the diluted brine from the SAM.

The actual operating pressures of the flash vessels in the MED system need to be established for the defined split ratio of 1.05. The pressure in the HP and MP stream were increased manually until no temperature crossover was detected. A minimum approach temperature of 10 ℃ was chosen for each of the heat exchangers. This temperature difference avoids unnecessarily large heat exchangers. The HP flash is operated at 2.0 bar, the MP flash at 0.5 bar and the LP at 0.09 bar. Without using MED, the heating requirements are ~25 MW, but splitting the stream into three stages and using heat integration opportunities results in a hot utility duty of only 8.9 MW (64 % reduction). After separating ethanol and water from the diluted stream from the SAM, the regenerated brine can be recycled and reused in the SAM [8].

4.2.4. *Ethanol preconcentration*

After the condensation part of PTD, the ethanol concentration is increased from 5 wt% in the fermentation broth to ~32 wt%. However, to obtain bioethanol that satisfies required standards (99.8 vol% in EU, 99.0 vol% in US and 99.6 vol% in Brazil [36]), additional purification is required. Due to the formation of azeotrope between ethanol and water (Table 2), several steps are needed in further processing. Firstly, the dilute ethanol – water mixture needs to be preconcentrated. At the industrial-scale, this step is usually performed by using conventional distillation [37]. Being a lower boiling component, ethanol is separated as a top product, together with some water due to the azeotrope formation. The highest ethanol concentration that can be obtained in this step is nearly the azeotropic one. Yet, approaching the azeotropic concentration in the top stream increases the energy requirements for this separation, but further purification to anhydrous product becomes less energy-demanding. The optimal ethanol concentration after the preconcentration has been determined to be 91 wt% ethanol [38]. This value was used subsequently.

Ethanol preconcentration takes place in distillation column C1 (see Fig. 9), operating at atmospheric pressure (1 bar). Sieve trays with a pressure drop of 8 mbar per tray were used as internals [39]. As the condensed ethanol – water mixture after the PTD is still at reduced pressure, simple pumps can be used to increase the pressure of this liquid stream to the atmospheric one. However, after increasing its pressure, the feed stream to column C1 is subcooled liquid resulting in larger

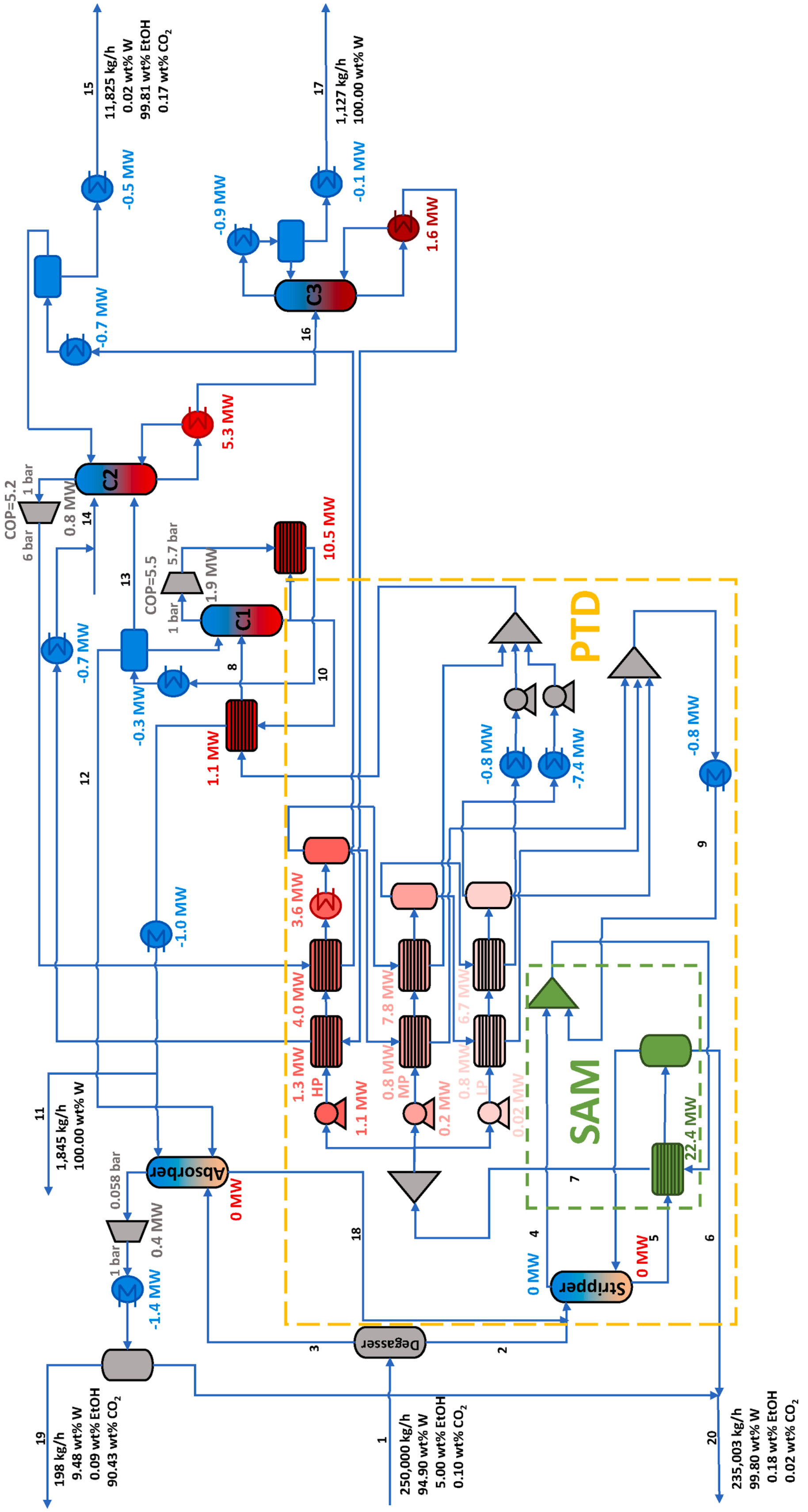

Fig. 11. Flowsheet of bioethanol recovery from the fermentation broth by process configuration 2 (PTD-MED) – heating duties (red and pink), cooling duties (blue), compressor/pump duties (grey), water (W), ethanol (EtOH), ethylene glycol (EG); condition and composition of numbered process streams are presented in Table 5.

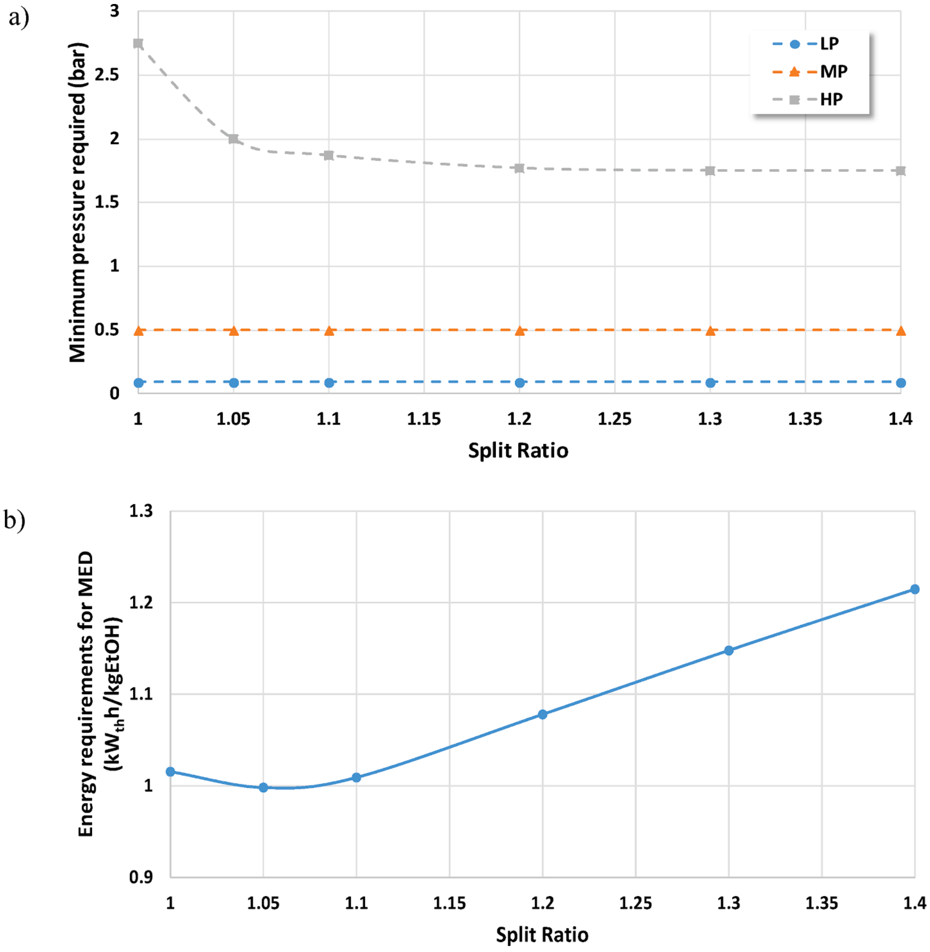

Fig. 12. A) minimum pressure required in each stream of the med system, b) energy requirements for med.

Table 2

Boiling points of ethanol and water, and azeotrope formation (at 1 bar).

Pure components		Azeotrope		
Component	Tb [°C]	Mass fraction	T [°C]	type
Ethanol	78.31	0.9557	78.15	homogenous
Water	100.00	0.0443		

heating duty requirements. The top product of this column is the pre-concentrated ethanol stream, while the bottom product is pure water. This water stream can be cooled and recycled to the fermenter in order to decrease the need for fresh water for the upstream part of the bio-ethanol production process. Consequently, this stream can be used to preheat the feed stream to column C1. Even though the described heat integration reduces the external heating requirements, still more than 10 MW (about 11.0 and 10.5 MW for PTD-VRC and PTD-MED, respectively) of heating duty is needed.

However, since this column is separating relatively close-boiling components, additional energy savings can be obtained by implementing mechanical vapor recompression (MVR). In this heat pumping method, vapor coming from the top of the distillation column is compressed and used to evaporate liquid from the bottom of the distillation column [40]. This results in significant reduction in need for external heating and cooling. By applying MVR to column C1, the need for external heating is completely avoided, while the need for external cooling is reduced by over 97 %. The coefficient of performance (COP), which is equal to the ratio of the upgraded heat (i.e. duty covered by the compressed vapor) and the required power (compression duty) [40], is around 5 (5.2 and 5.5 for PTD-VRC and PTD-MED, respectively), thus proving significant energy savings. The compression ratio that is needed for these MVR systems is about 6.4 for PTD-VRC and 5.6 for PTD-MED, meaning that multi-stage compressors should be used.

To obtain a high purity final bioethanol product, a partial condenser was considered for column C1 to remove the remaining CO_2 in the ethanol – water mixture. However, this would lead to more ethanol being lost with CO_2. Fig. 13 shows that to obtain 99.8 wt% ethanol, a vapor fraction of 0.1 on a mass basis is needed in a C1 partial condenser, resulting in recovery of only ~81 % ethanol. However, this significant loss of product was not considered satisfactory and further modifications in process design were conducted.

To avoid losing a significant amount of ethanol, an additional absorption column has been included. The bottom product (water) from column C1 is firstly used to preheat the feed stream to this column. Afterwards, part of this water stream is used to absorb ethanol from CO_2-rich vapor streams from both the degasser unit and the C1 partial condenser. The top product from this column is a vapor stream containing mostly water and CO_2. Water from this stream is condensed, mixed with the stream containing microorganisms and recycled to the fermenter, while the remaining CO_2-rich vapor stream is released from the process. As this CO_2 is emitted into the atmosphere, it was accounted for in the sustainability assessment, as described in a later section. The bottom product from this stripping column is water and ethanol stream that is being sent to the stripping column before the SAM unit. Including this additional column in the process design significantly reduces the amount of lost ethanol in the CO_2-rich streams, from ~14 % to less than 0.002 % of the initially present ethanol. As the added absorption column does not require any external heating, the overall energy requirements

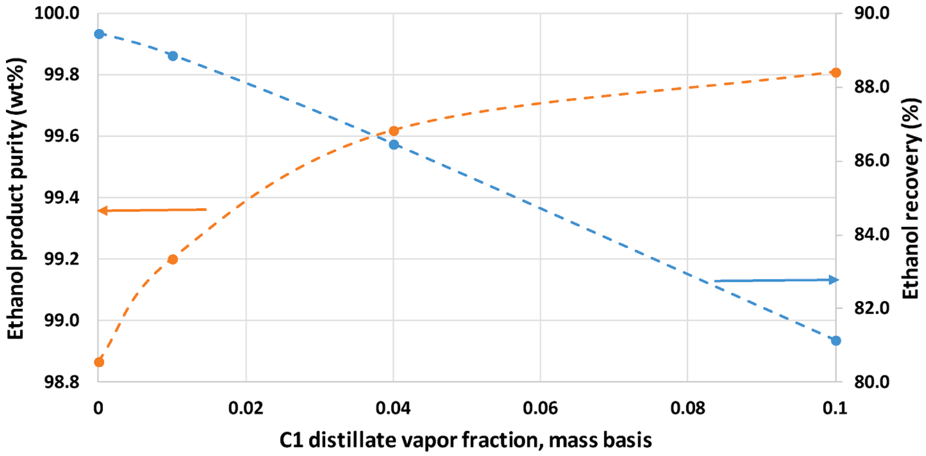

Fig. 13. Dependency of ethanol product purity and recovery on the vapor fraction in C1 partial condenser.

are not increased. Due to the reduced operating pressure of this column, structured packing (type Sulzer Mellapak 250) was chosen as internals, with a pressure drop of 0.225 mbar per theoretical stage [33].

4.2.5. *Ethanol dehydration*

The distillate product from the C1 preconcentration column needs to be further dehydrated to obtain an on-spec product. On industrial-scale, the most common dehydration techniques are extractive distillation, azeotropic distillation and adsorption on zeolite [37]. Adsorption is not a proper method in this case since a rather large amount of zeolite is needed due to the large flowrates in the considered process design. With an average adsorption capacity in the range of 0.011–0.387 $g_{water}/g_{zeolite}$ [41], about 24–848 $tonne_{zeolite}$ is needed for 8 h operation (for the considered capacity). Furthermore, azeotropic distillation has several disadvantages compared to extractive distillation for large-scale ethanol dehydration: larger solvent flowrates are needed, energy requirements are higher since all added solvent needs to be completely evaporated [42] and the required control system is more complicated [43]. Therefore, extractive distillation (ED) is often chosen as the best option for ethanol dehydration at an industrial level [36]. In this dehydration method, a high-boiling solvent is added to the ethanol – water mixture. This solvent changes relative volatility of the components, without forming azeotropes with any of them [44]. Ethylene glycol is commonly used as solvent for the large-scale ethanol dehydration by extractive distillation [37]. Overall, as ED with ethylene glycol had been proven to be the most effective method for ethanol dehydration, it was chosen for the final purification step.

This process is performed in extractive distillation column C2 and solvent recovery column C3 that operate at atmospheric pressure (1 bar). Sieve trays (with a pressure drop of 8 mbar per tray) were considered as internals [39]. A solvent-to-feed mass ratio of 1.2 was used since it has been determined to be the optimal one for the ethanol dehydration part of the process [45]. The top product from the ED column C2 is a high-purity (99.8 wt%) bioethanol product, while the bottom product containing solvent and water is sent to the solvent recovery column C3. Pure water, separated as the top product from column C3, can be cooled down and recycled to the fermenter to reduce fresh water requirements for this step. The bottom product is recovered solvent that is being recycled and reused in column C2.

Having designed also the ethanol dehydration part of the process, additional energy savings can be obtained by using heat integration opportunities. The complete ethanol recovery process with applying heat pump assisted desorption step (PTD-VRC) and MED (in PTD-MED) were designed and their performance is compared in the following sections.

4.2.6. *Process design of the full bioethanol recovery*

Configuration 1 – PTD with heat pump assisted desorption (PTD-VRC)

The flowsheet of the overall process is presented in Fig. 9, and the design parameters for the distillation columns are summarized in Table 3, while the main streams are given in Table 4.

As the temperature at the top and bottom of extractive distillation column C2 are 76 °C and 155 °C, respectively, compressing the top vapor would not provide sufficient heat to the reboiler. Nonetheless, a side reboiler (1.9 MW) can be added wherein the compressed top vapor is used to evaporate part of the liquid side stream. Using this heat integration, the heating duty for column C2 is reduced by about 36 % (from 5.3 MW to 3.4 MW). Additionally, the external cooling for this column is decreased by 37 % (from −3.8 MW to −2.4 MW). The COP of this heat pump system is about 2.9. Since this value is higher than the ideal COP of an industrial heat pump (starting from 2.0 [46]) and also higher than the conservative value of thermal-electrical conversion factor (about 2.5 [47]), the proposed heat pump system can reduce the total energy requirements for this column leading to energy savings. As the required compression ratio is 5.0, a multi-stage compressor should be used.

Furthermore, since the recovered ethylene glycol from the bottom of column C3 must be cooled before being reused in extractive distillation column C2 [38], it can be utilized to evaporate part of the bottom liquid from column C2. Even though the recovered solvent cannot provide sufficient heat to eliminate the need for heating utilities for column C2, this heat integration results in additional 21 % reduction in external heating requirements. As a result of the described heat integrations, the total need for external heating for the extractive distillation column is reduced by about 57 % (from 5.3 MW to 2.3 MW).

Moreover, additional heat integration can be applied to improve the performance of the desorption part of the PTD process. The bottom product (water) from the preconcentration column C1 can evaporate part of ethanol and water from diluted brine before being used to absorb ethanol from CO_2-rich streams. By this heat integration, the required heating duty for the desorption step is reduced by ~0.8 MW. Additionally, the recovered solvent needs to be further cooled even after being used to evaporate part of the bottom liquid from the extractive distillation column C2 [38]. Consequently, it can also be used to evaporate part of the diluted brine and to reduce the total heating duty for the desorption step by an additional 0.8 MW. Therefore, using the heat content of hot process streams in the desorption step can reduce the total heating requirements by more than 6 %. Although this reduction is not that large, the compressor duty decreases by about 7 % (from 3.7 MW to 3.4 MW) and the outlet temperature of the compressed vapor decreases from 254 °C to 242 °C. The COP for the vapor recompression system is ~6.9, while the compression ratio is 4.0. Accordingly, the described heat

Table 3
Design parameters of the distillation columns (before enhancing the processes with heat pumping and heat integration).

Distillation column	Stripping column	Preconcentration column C1	Extractive distillation column C2	Solvent recovery column C3	Ethanol absorption column
Process configuration 1 – PTD-VRC					
Number of stages[*]	10	30	32	16	30
Feed stage	1 (broth) 10 (vapor)	15	4 (solvent) 24 (91 % ethanol)	8	
Top/bottom pressure [bar]	0.052/0.054	1/1.232	1/1.248	1/1.120	0.058/0.065
Top/bottom temperature [°C]	30.7/33.9	75.9/105.6	75.6/154.5	99.5/199.0	34.6/32.6
Reboiler/Condenser duty [MW]	0/0	11.0/−9.7	5.3/−3.8	1.6/−0.9	0/0
Reflux ratio, mass	/	1.54	0.35	0.31	/
Column diameter [m]	4.5	2.3	1.4	0.9	1.2
Process configuration 2 – PTD-MED					
Number of stages[*]	10	30	32	16	30
Feed stage	1 (broth) 10 (vapor)	15	4 (solvent) 24 (91 % ethanol)	8	
Top/bottom pressure [bar]	0.052/0.054	1/1.232	1/1.248	1/1.120	0.058/0.065
Top/bottom temperature [°C]	30.7/33.9	75.8/105.6	75.5/154.5	99.6/200.0	34.8/32.6
Reboiler/Condenser duty [MW]	0/0	10.5/−9.5	5.3/−3.9	1.6/−0.9	0/0
Reflux ratio, mass	/	1.53	0.40	0.32	/
Column diameter [m]	4.5	2.2	1.4	0.9	1.2

[*] By convention in Aspen Plus, the 1st stage is the condenser (if there is a condenser) and the last stage is the reboiler (if there is a reboiler).

Table 4
Conditions and compositions of the main streams (configuration 1, PTD-VRC).

Stream	1	2	3	4	5	6	7	8	9	10
Temperature [C]	37.0	33.9	33.9	30.7	33.9	34.1	40.8	79.8	50.0	105.6
Pressure [bar]	1.000	0.065	0.065	0.052	0.054	0.054	0.054	1.112	0.054	1.232
Flowrate [kg/hr]	250,000	248,279	1,721	41,292	266,799	233,132	96,864	41,292	55,572	26,551
Flowrate [ktonne/y]	2,000.0	1,986.2	13.8	330.3	2,134.4	1,865.1	774.9	330.3	444.6	212.4
Mass fractions										
Water	0.9490	0.9513	0.6141	0.6738	0.9960	0.9982	0.5587	0.6738	0.4731	1.0000
Ethanol	0.0500	0.0482	0.3144	0.3227	0.0040	0.0018	0.1415	0.3227	0.0069	0.0000
LiBr	0.0000	0.0000	0.0000	0.0000	0.0000	0.0000	0.2983	0.0000	0.5199	0.0000
CO_2	0.0010	0.0005	0.0715	0.0035	0.0000	0.0000	0.0015	0.0035	0.0000	0.0000
Ethylene glycol	0.0000	0.0000	0.0000	0.0000	0.0000	0.0000	0.0000	0.0000	0.0000	0.0000
Stream	11	12	13	14	15	16	17	18	19	20
Temperature [C]	37.0	75.9	75.9	60.0	30.0	154.5	37.0	32.6	60.7	33.8
Pressure [bar]	1.232	1.000	1.000	1.120	1.000	1.248	1.000	0.065	1.000	0.054
Flowrate [kg/hr]	1,551	1,474	13,267	15,288	12,102	16,438	1,151	26,144	206	234,977
Flowrate [ktonne/y]	12.4	11.8	106.1	122.3	96.8	131.5	9.2	209.2	1.6	1,879.8
Mass fractions										
Water	1.0000	0.0722	0.0879	0.0010	0.0002	0.0708	0.9992	0.9312	0.0937	0.9980
Ethanol	0.0000	0.8424	0.9106	0.0000	0.9981	0.0000	0.0008	0.0681	0.0010	0.0018
LiBr	0.0000	0.0000	0.0000	0.0000	0.0000	0.0000	0.0000	0.0000	0.0000	0.0000
CO_2	0.0000	0.0854	0.0015	0.0000	0.0016	0.0000	0.0000	0.0000	0.9053	0.0002
Ethylene glycol	0.0000	0.0000	0.0000	0.9990	0.0001	0.9291	0.0000	0.0007	0.0000	0.0000

integrations lead to a safer and less energy-intensive bioethanol recovery process.

Configuration 2 – PTD combined with multi-effect distillation (PTD-MED)

The overall flowsheet is presented in Fig. 11, while the design parameters for the distillation columns are given in Table 3, and the main streams are listed in Table 5. The largest heating duty in this process configuration is the one needed to evaporate part of the HP stream in the MED process (about 9.0 MW). Therefore, additional heat integration and heat pumping were applied to decrease energy requirements for this step. Firstly, the recovered ethylene glycol from the bottom of column C3 is used to heat part of the HP stream, which decreases external heating requirements by about 1.3 MW. Secondly, top vapor from extractive distillation column C2 is compressed and also used to evaporate part of the HP stream. This implementation of heat pumping reduced external heating requirements by additional 4.0 MW, having a COP of 5.2, which confirms the large energy savings. The compression ratio needed for this heat pump system is 6.0, which indicates that a multi-stage compressor should be used. Overall, the external heating for the MED part of the process is reduced by about 60 % (from 8.9 MW to 3.6 MW).

4.3. *Economic evaluation*

To evaluate the performance of the designed processes, a complete economic analysis was performed. The published NREL methodology [48] was used to calculate both the capital (CAPEX) and operating (OPEX) expenditures, considering an operating time of 8,000 h per year.

Table 5
Conditions and compositions of the main streams (configuration 2, PTD-MED).

Stream	1	2	3	4	5	6	7	8	9	10
Temperature [℃]	37.0	33.9	33.9	30.7	33.9	34.1	40.8	85.1	50.0	105.6
Pressure [bar]	1.000	0.065	0.065	0.052	0.054	0.054	0.054	1.370	0.054	1.232
Flowrate [kg/hr]	250,000	248,279	1,721	41,237	266,495	232,868	96,836	41,236	55,598	26,845
Flowrate [ktonne/y]	2,000.0	1,986.2	13.8	329.9	2,132.0	1,862.9	774.7	329.9	444.8	214.8
Water	0.9490	0.9513	0.6141	0.6741	0.9960	0.9982	0.5578	0.6809	0.4715	1.0000
Ethanol	0.0500	0.0482	0.3144	0.3224	0.0040	0.0018	0.1423	0.3156	0.0088	0.0000
LiBr	0.0000	0.0000	0.0000	0.0000	0.0000	0.0000	0.2984	0.0000	0.5197	0.0000
CO_2	0.0010	0.0005	0.0715	0.0035	0.0000	0.0000	0.0015	0.0035	0.0000	0.0000
Ethylene glycol	0.0000	0.0000	0.0000	0.0000	0.0000	0.0000	0.0000	0.0000	0.0000	0.0000
Stream	11	12	13	14	15	16	17	18	19	20
Temperature [℃]	37.0	75.8	75.8	60.0	30.0	154.5	37.0	32.6	60.5	33.8
Pressure [bar]	1.232	1.000	1.000	1.120	1.000	1.248	1.000	0.065	1.000	0.054
Flowrate [kg/hr]	1,845	1,439	12,952	14,740	11,825	15,866	1,127	25,826	198	235,003
Flowrate [ktonne/y]	14.8	11.5	103.6	117.9	94.6	126.9	9.0	206.6	1.6	1,880.0
Mass fractions										
Water	1.0000	0.0717	0.0872	0.0001	0.0002	0.0711	1.0000	0.9315	0.0948	0.9980
Ethanol	0.0000	0.8416	0.9112	0.0000	0.9981	0.0000	0.0000	0.0678	0.0009	0.0018
LiBr	0.0000	0.0000	0.0000	0.0000	0.0000	0.0000	0.0000	0.0000	0.0000	0.0000
CO_2	0.0000	0.0868	0.0015	0.0000	0.0017	0.0000	0.0000	0.0000	0.9043	0.0020
Ethylene glycol	0.0000	0.0000	0.0000	0.9999	0.0000	0.9289	0.0000	0.0007	0.0000	0.0000

The total CAPEX includes costs related to equipment purchase and installation, but also expenses due to home office and construction, site development, additional piping, project contingency, working capital, warehouse, field and prorateable expenses. The estimation of the equipment costs for every process unit was performed using the suggested correlations [49]. Marshall and Swift cost index of 1,638.2 (end of 2018) was used in these estimations [50]. The total OPEX was determined considering costs for utilities, labor, maintenance and property insurance [48]. Costs for utilities were estimated following an approximation [49] that takes into account: 60.48 $/MWh for electricity, 28.01 $/MWh for low-pressure steam, 29.59 $/MWh for medium-pressure steam, 35.57 $/MWh for high-pressure steam, 1.27 $/MWh for cooling water, 15.95 $/MWh for chilled water. Additionally, reliable market data were utilized to calculate capital and energy costs for vacuum pumps needed in the designed processes [51]. Total annual costs (TAC) were calculated to take into account both CAPEX and OPEX, with assumed payback period of 10 years as recommended by the NREL methodology [48]. Additionally, the minimum added price for the bioethanol recovery was estimated using the literature recommendations from the same source [48]. More details about the followed methodology for economic assessment is presented in the Supplementary Information file.

The calculated economic indicators for both configurations of the bioethanol recovery process are summarized in Table 6. The total cost for installing all process equipment units is 18,213 k$ for PTD-VRC and 15,470 k$/y for PTD-MED. The cost distribution between different equipment types is presented in Fig. 14. For PTD-VRC, the largest part of equipment cost is the cost for compressors (~55 %) and heat exchangers (~28 %), whereby the costs for distillation columns, pumps and flash vessels are significantly lower (respectively 13 %, 3 % and 1 %). In the case of PTD-MED, by far the biggest part of equipment expenses is the cost for heat exchangers (~37 %) and compressors (~34 %), followed by the cost for distillation columns (~16 %) and pumps (~11 %), while the cost for flash vessels is significantly lower (only ~2 %). CAPEX is 33,595 k$ for PTD-VRC and 28,378 k$ for PTD-MED. The equipment costs are the largest contributor to the CAPEX in both process configurations (about 54–55 %, shown in Fig. 14).

Table 6
Key performance indicators in terms of economics and sustainability.

	Process configuration 1 (PTD-VRC)	Process configuration 2 (PTD-MED)
Economic indicators		
CAPEX [k$]	33,595	28,378
OPEX [k$/y]	8,481	9,512
OPEX [$/$kg_{EtOH}$]	0.088	0.101
TAC [k$/y]	11,840	12,349
TAC [$/$kg_{EtOH}$]	0.122	0.131
Added selling price [$/$kg_{EtOH}$]	0.134	0.141
Sustainability metrics		
Thermal energy requirements [$kW_{th}h/kg_{EtOH}$]	0.320	0.889
Electrical energy requirements [$kW_{e}h/kg_{EtOH}$]	0.561	0.378
Primary energy requirements [$kW_{th}h/kg_{EtOH}$]	1.723	1.834
Water consumption [m^3_w/kg_{EtOH}]	0.158	0.234
Water loss [m^3_w/kg_{EtOH}]	0.011	0.016
CO_2 emissions [kg_{CO2}/kg_{EtOH}]*	0.292/0.035	0.309/0.136
Material intensity [kg_{waste}/kg_{EtOH}]	0.000	0.000
Pollutant emissions [$kg_{pollutant}/kg_{EtOH}$]**	0.000	0.000
Toxic emissions [$kg_{toxic\ materal}/kg_{EtOH}$]**	0.000	0.000

* Grey/green electricity.
** Excluding emitted CO_2.

OPEX for both process configurations is also presented in Fig. 14. OPEX for PTD-VRC is 8,481 k$/y, which is mostly due to the cost for utilities (~57 %) and operating labor (~35 %). The high electricity cost (~39 % of the total OPEX) is mainly due to the usage of compressors (accounting together ~96 % of the electricity cost), whereby the electricity cost for pumps is significantly lower (~4%). In case of PTD-MED, OPEX is 9,512 k$/y. The largest part of the OPEX is the cost for utilities (over 62 %) and operating labor (~31 %). Among the cost for utilities, the largest distribution is due to the different types of heating utilities (together ~ 38 % of the total OPEX). Expressed in relative terms, the

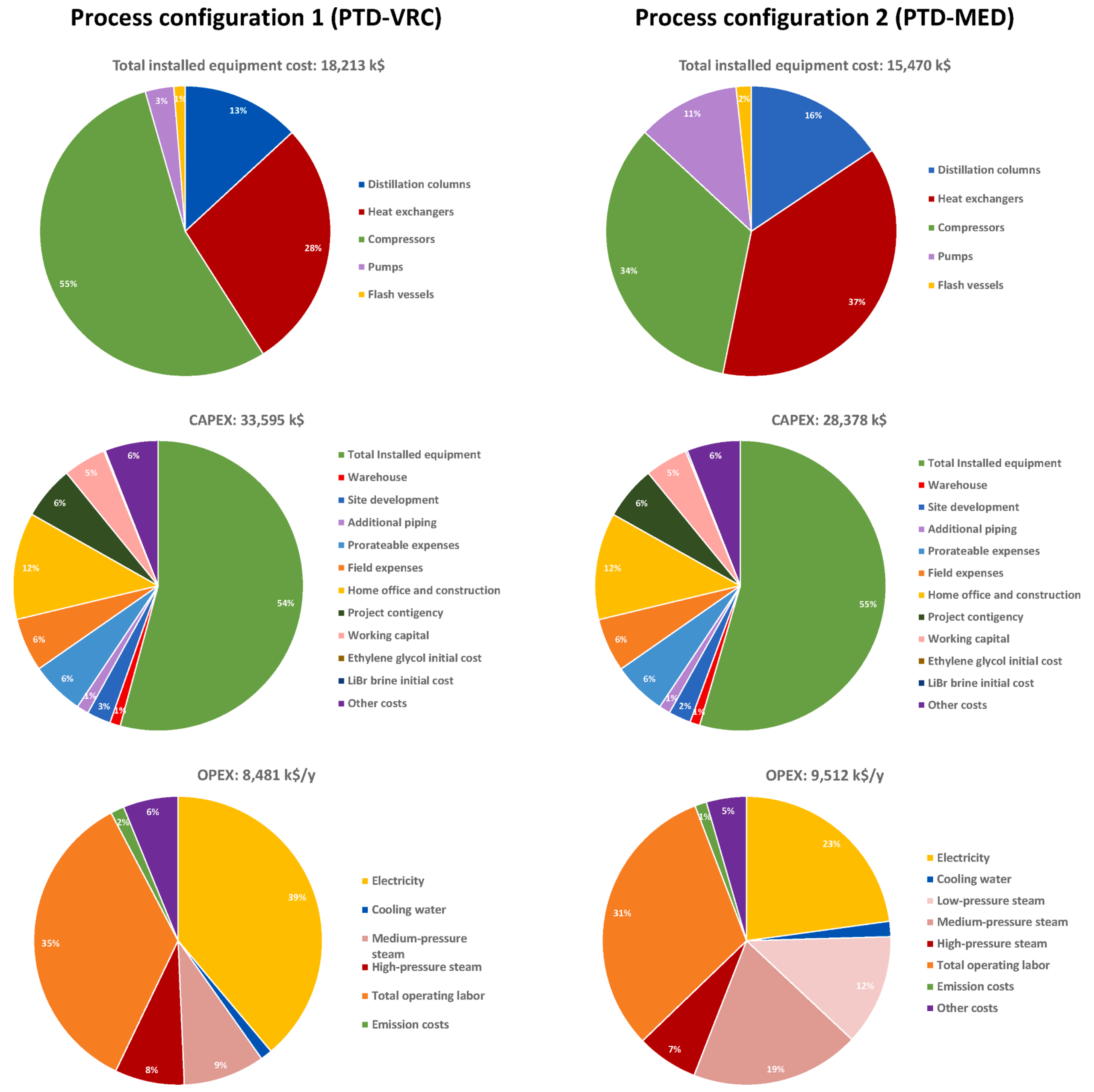

Fig. 14. Total installed equipment cost, CAPEX and OPEX for bioethanol recovery processes.

OPEX for two process configurations are 0.088 and 0.101 $/kg$_{\mathrm{EtOH}}$, respectively.

When both CAPEX and OPEX are taken into account, the TAC for the bioethanol recovery process is 11,840 k$/y for PTD-VRC and 12,349 k$/y for PTD-MED, which amounts to 0.122 and 0.131 $/kg$_{\mathrm{EtOH}}$ respectively. Thus, the minimum added price for the bioethanol recovery process in case of PTD-VRC is 0.134 $/kg$_{\mathrm{EtOH}}$, while for the PTD-MED process configuration the value is 0.141 $/kg$_{\mathrm{EtOH}}$. The economic assessments of the developed process configurations prove the competitiveness of the proposed designs for the large-scale bioethanol recovery from the fermentation broth [38,42,45].

Summing up, the PTD-MED system requires less investment, but the PTD-VRC option is more favorable in terms of operating costs. The effect of the assumed payback period on the TAC for both process configurations is presented in Fig. 15. For a payback period of less than 3.5 years, PTD-MED is more economically favorable, but if the payback period exceeds 3.5 years, using PTD-VRC leads to a much lower TAC.

However, due to the large contribution of utilities to the OPEX, the availability and cost of certain types of utilities must be determined per site prior to choosing the best option. If the price ratio for heating utilities (steam) to electricity is smaller than currently assumed (conversion factor 2.5), then PTD-MED is more likely to become the better solution for the PTD process. This is due to the fact that expense ratio for heating utilities to electricity is currently ~38/23 for this case, while for the PTD-VRC option this ratio is ~17/39.

4.4. Sustainability assessment

In addition to the economic analysis, a significant focus was put on evaluating the performance of the designed recovery processes in terms of environmental impact. Table 6 summarizes the main sustainability metrics [52] for both process configurations of the bioethanol recovery from the fermentation broth.

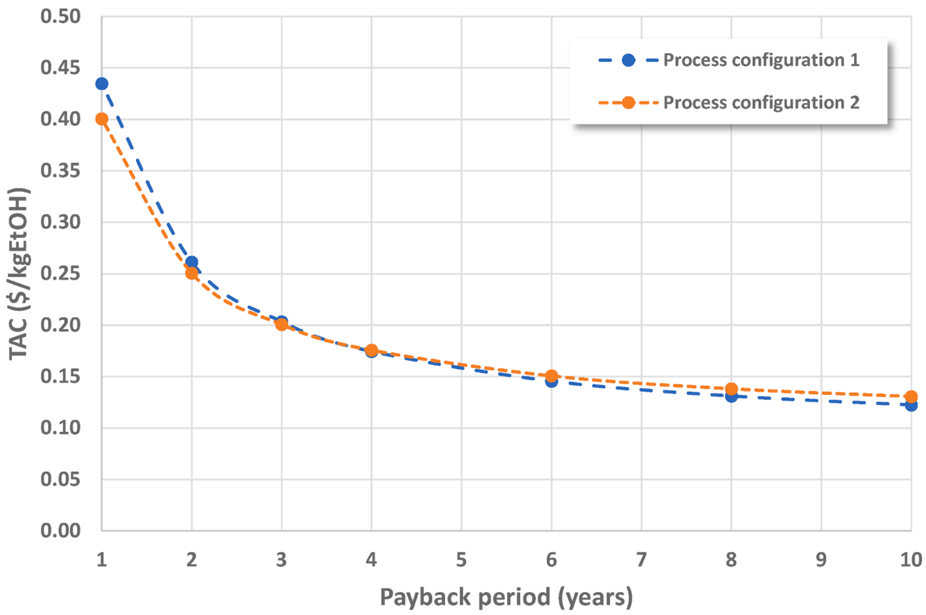

Fig. 15. Effect of payback period on the specific total annual cost.

- ***Energy intensity*** is a measure of total energy, both thermal and electrical, expressed per kilogram of product [52]. Inefficiencies in power generation are taken into account through a thermal-electrical conversion factor that quantifies heat needed to produce a unit of electrical output. This factor is commonly expressed as ratio of heat input to electrical output. By using thermal-electrical conversion factor, all losses in electricity generation and distribution are taken into account. Following recommendations from several sources [47,53], a rather conservative value of 2.5 for this factor is considered in the calculation of primary energy requirements. The thermal energy requirements account for all heating utilities (low-, medium- and high-pressure steam) but of course, do not account for the thermal energy that is recovered with process-process heat exchangers (not using utilities). Thus, 0.320 $kW_{th}h/kg_{EtOH}$ is needed in PTD-VRC process and 0.889 $kW_{th}h/kg_{EtOH}$ is needed in PTD-MED process. Higher usage of thermal energy for PTD-MED is mostly due to the need for external heating in the MED section. The electrical energy requirements are 0.561 $kW_{e}h/kg_{EtOH}$ (PTD-VRC) and 0.378 $kW_{e}h/kg_{EtOH}$ (PTD-MED). The larger electrical energy requirement for PTD-VRC is mainly due to the compressor used in the heat pump assisted desorber unit. The overall primary energy requirements (considering both the thermal and electrical energy usage) are 1.723 and 1.834 $kW_{th}h/kg_{EtOH}$ for PTD-VRC and PTD-MED, respectively. The performed analysis of energy requirements has demonstrated that both designed bioethanol recovery processes are highly competitive for the large-scale operation [38,42,45].
- ***Water consumption*** presents the amount of fresh water needed per kilogram of product [54]. This accounts for the cooling water, loss of cooling water, and loss of steam condensate. Common estimations are that about 7 % of cooling water is lost in cooling towers due to evaporation and misting losses [52], and practically about 70 % of steam condensate can be recovered due to the inefficiencies in steam generation and usage [55]. The total need for cooling water is 0.147 m_w^3/kg_{EtOH} for PTD-VRC and 0.218 m_w^3/kg_{EtOH} for PTD-MED. Taking into account loss of both cooling water and steam condensate, the total need for water for two process configurations is 0.158 and 0.234 m_w^3/kg_{EtOH}, respectively. Furthermore, about 0.011 m_w^3/kg_{EtOH} of water is lost with the bioethanol recovery in PTD-VRC, whereby the total water losses in PTD-MED are 0.016 m_w^3/kg_{EtOH}.
- ***Material intensity*** is a measure of total waste formed per kilogram of product [52]. In addition to high-purity bioethanol product, the output streams from both process configurations are the stream containing living microorganisms and heavy inert components that might be recycled to the fermenter, and water streams that are cooled and also may be recycled to the fermenter. Furthermore, the recovered LiBr brine and ethylene glycol are being reused in the process. Lastly, the CO_2-rich stream that is emitted was accounted for in the greenhouse gas emissions metrics and therefore it was not considered here. Since no stream is waste, the material intensity for both designed configurations equals zero.
- ***Greenhouse gas emission*** is expressed as the amount of CO_2 emitted per kilogram of product [54]. Recommendations from the published literature were used when calculating this sustainability metrics [50,56]. To estimate CO_2 emissions as accurately as possible, emphasize was put on the source of electricity used. A distinction was made between electricity obtained from fossil fuels (grey electricity) and electricity from renewable sources (green electricity). Additionally, the CO_2 that was evaporated from the fermentation broth was taken into account in these calculations. If grey electricity is used, the total CO_2 emissions are 0.292 kg_{CO2}/kg_{EtOH} for PTD-VRC and 0.309 kg_{CO2}/kg_{EtOH} for PTD-MED. However, if green electricity is used, the total CO_2 emissions for PTD-VRC are reduced by ~88 % to only 0.035 kg_{CO2}/kg_{EtOH}, whereas for PTD-MED this reduction is ~56 % to 0.136 kg_{CO2}/kg_{EtOH}.
- ***Pollutant and toxic emissions*** present the amount of different pollutants and toxic materials formed per kilogram of product [52]. Besides the already mentioned CO_2, the bioethanol recovery from fermentation broth does not emit any other pollutants or toxic materials.

4.5. PTD technology perspectives

Pass-through distillation is a new method that should certainly be added to the separation technologies toolbox, being useful in applications where classic distillation is not suitable and other methods are either too costly or too prone to fouling.

PTD can be applied not only to the recovery of bio-alcohols, but also to the processing of complex aqueous waste streams, which are too contaminated to be treated and are presently incinerated at great cost. Other applications may include: organic solvents recovery, water removal for drying of chemicals, aroma recovery in the food industry, concentrating orange juice, separation of heat-sensitive materials, purification of pharmaceutical products, etc.

As proven in this study, PTD can also be coupled with advanced heat pumping systems or MED to reduce total energy requirements, resulting in an overall highly competitive downstream process. Performing evaporation and condensation at different pressures offers several advantages as compared to conventional vacuum distillation:

- Applicability of this technology is expanded to highly heat-sensitive materials.
- Usage of expensive refrigeration is avoided, potentially resulting in significantly lower operating costs [8].
- Equipment size is reduced as compared to conventional distillation columns [8].
- The field of application can be extended to new processes, e.g. ethanol recovery from fermentation broth. Continuous separation of fermentation products will significantly reduce end-product inhibition and thus increase fermentation yield. Furthermore, keeping temperatures below 37 °C allows the recycling of present microorganisms to the fermenter. Significant biomass loss can be avoided in this way, while allowing fermentation to be performed in a closed loop [8].

Even though PTD technology has some limitations (e.g. difficulties in finding appropriate absorption fluids, or properly modeling the thermodynamic properties), and might not be suitable for every application, its effectiveness has been demonstrated in situations where water serves as the primary volatile component and lithium bromide solution functions as the absorbent fluid [8]. While it may not be the best technology for large-scale ethanol recovery, it is proven to be highly competitive and effective [37] hence it should be added to the separation methods toolbox. Additionally, the usage of PTD may be even more beneficial in the case of more volatile products than ethanol, which would otherwise lead to lower condensation temperatures in the initial separation step. Further research is needed to determine other combinations of volatile components and absorbent fluids. More information about the PTD technology is available on the websites: *https://www.ptdistil.com* and *https://www.drystill.ca*.

5. Conclusions

The main innovations in this original research are multifaceted. One novelty is related to the rigorous modeling of the complex ternary system LiBr – ethanol – water. A reliable property model was developed to account for interactions between the present electrolyte and two solvents, as well as relations among two polar solvents. Another novelty consists in the implementation of pass-through distillation (PTD) technology for industrial-scale bioethanol recovery from the dilute fermentation broth.

The proposed PTD process can effectively recover more than 94 % of ethanol from the fermentation broth, while concentrating the water – ethanol mixture from 5 wt% to over 30 wt% and providing full recycle of biomass. The flexibility of PTD technology was expanded by developing and comparing two designs for the desorption and the condensation parts: heat pump (vapor recompression) assisted desorber (PTD-VRC) and multi-effect distillation (PTD-MED). Also, the preconcentration and dehydration sections were designed for both options to obtain high-purity (99.8 wt%) bioethanol.

The performed analysis of economic and environmental impacts proved that PTD is a competitive technology that can be used in large-scale concurred alcohol recovery and fermentation (0.122 $\$/\mathrm{kg}_{\mathrm{EtOH}}$ and 1.723 $\mathrm{kW}_{\mathrm{th}}\mathrm{h}/\mathrm{kg}_{\mathrm{EtOH}}$ for PTD enhanced with heat pumps, and 0.131 $\$/\mathrm{kg}_{\mathrm{EtOH}}$ and 1.834 $\mathrm{kW}_{\mathrm{th}}\mathrm{h}/\mathrm{kg}_{\mathrm{EtOH}}$ for PTD coupled with multi-effect distillation). Apart from removing inhibitory product from the broth, recycling the separated microorganisms with most of the water may enhance the fermentation process by avoiding loss of biomass and reducing water requirements. As both options proved to be cost-effective and energy-efficient, the choice of the best configuration depends on the exact site location and the availability of different utilities.

As PTD has already been proven to be efficient on bench- and pilot-scale levels by Drystill, this original research offers insights into the application of this novel technology on an industrial-level. Further research which explores the application of the PTD process to other systems would be extremely beneficial. Species which require refrigeration for condensation as well as thermally unstable components are an important direction in which to focus future research.

CRediT authorship contribution statement

Tamara Janković: Writing – review & editing, Writing – original draft, Visualization, Validation, Software, Methodology, Data curation, Conceptualization. **Adrie J.J. Straathof:** Writing – review & editing, Validation, Supervision, Methodology, Formal analysis, Conceptualization. **Ian R. McGregor:** Writing – review & editing, Validation, Methodology, Formal analysis. **Anton A. Kiss:** Writing – review & editing, Writing – original draft, Visualization, Validation, Supervision, Resources, Project administration, Methodology, Investigation, Formal analysis, Conceptualization.

Declaration of competing interest

The authors declare that they have no known competing financial interests or personal relationships that could have appeared to influence the work reported in this paper.

Data availability

Data will be made available on request.

Acknowledgements

All persons who have made substantial contributions to the work reported in the manuscript (e.g., technical help, writing and editing assistance, general support), but who do not meet the criteria for authorship, are named in the Acknowledgements and have given us their written permission to be named. If we have not included an Acknowledgements, then that indicates that we have not received substantial contributions from non-authors.

Appendix A. Supplementary data

Supplementary data to this article can be found online at https://doi.org/10.1016/j.seppur.2024.126292.

References

[1] L.M. Vane, Separation technologies for the recovery and dehydration of alcholos from fermentation broths, Biofuels, Bioproducts and Biorefining. 2 (2008) 553–588, https://doi.org/10.1002/bbb.108.

[2] H.-J. Huang, S. Ramaswamy, U.W. Tschirner, B.V. Ramarao, A review of separation technologies in current and future biorefineries, Separation and Purification Technology. 62 (2008) 1–21, https://doi.org/10.1016/j.seppur.2007.12.011.

[3] C.A. Cardona, Ó.J. Sánchez, Fuel ethanol production: Process design trends and integration opportunities, Bioresource Technology. 98 (2007) 2415–2457, https://doi.org/10.1016/j.biortech.2007.01.002.

[4] R. Liu, F. Shen, Impacts of main factors on bioethanol fermentation from stalk juice of sweet sorghum by immobilized Saccharomyces cerevisiae (CICC 1308), Bioresource Technology. 99 (2008) 847–854, https://doi.org/10.1016/j.biortech.2007.01.009.

[5] I. McGregor, S. Furlong, Concurrent Alcohol Recovery and Fermentation Using Pass-Through Distillation, Industrial Biotechnology. 13 (2017) 107–112, https://doi.org/10.1089/ind.2017.29081.imc.

[6] A.A. Kiss, J.P. Lange, B. Schuur, D.W.F. Brilman, A.G.J. van der Ham, S.R. A. Kersten, Separation technology–Making a difference in biorefineries, Biomass and Bioenergy. 95 (2016) 296–309, https://doi.org/10.1016/j.biombioe.2016.05.021.

[7] G.M. Bollas, C.C. Chen, P.I. Barton, Refined electrolyte-NRTL model: Activity Coefficient Expressions for Application to Multi-Electrolyte Systems, AIChE Journal. 54 (2008) 1608–1624, https://doi.org/10.1002/aic.11485.

[8] A.A. Kiss, I.R. McGregor, S. Furlong, Pass-through distillation - A new player in separation technology, NPT Procestechnologie. 4 (2014).

[9] A.C. Dimian, C.S. Bildea, A.A. Kiss, Integrated Process and Product Design, Computer Aided Process Engineering. 35 (2014).

[10] A.A. Kiss, J. Grievink, M. Rito-Palomares, A systems engineering perspective on process integration in industrial biotechnology, Journal of Chemical Technology and Biotechnology. 90 (2015) 349–355, https://doi.org/10.1002/jctb.4584.

[11] J. Pátek, J. Klomfar, Solid-liquid phase equilibrium in the systems of LiBr-H2O and LiCl-H2O, Fluid Phase Equilibria. 250 (2006) 138–149, https://doi.org/10.1016/j.fluid.2006.09.005.

[12] M.R. Conde, Properties of aqueous solutions of lithium and calcium chlorides: Formulations for use in air conditioning equipment design, International Journal of Thermal Sciences. 43 (2004) 367–382, https://doi.org/10.1016/j.ijthermalsci.2003.09.003.

[13] I.R. McGregor, C.H. Belchers, Stripping absorption module, US 8,757,599 B2, 2014.

[14] C. Somers, A. Mortazavi, Y. Hwang, R. Radermacher, P. Rodgers, S. Al-Hashimi, Modeling water/lithium bromide absorption chillers in ASPEN Plus, Applied Energy. 88 (2011) 4197–4205, https://doi.org/10.1016/j.apenergy.2011.05.018.

[15] R.H. Perry, D.W. Green, Distillation, in: Perry's Chemical Engineering Handbook, McGraw-Hill, 1997: pp. 13–10.

[16] N. Hu, D.W. Schaefer, Effect of impurity compounds on ethanol hydration, Journal of Molecular Liquids. 155 (2010) 29–36, https://doi.org/10.1016/j.molliq.2010.05.001.

[17] K.R. Patil, A.D. Trlpathi, G. Pathak, S.S. Katti, Thermodynamic Properties of Aqueous Electrolyte Solutions. 1. Vapor Pressure of Aqueous Solutions of LiCl, LiBr and LiI, Journal of Chemical and Engineering Data. 35 (1990) 166–168.

[18] K. Nasirzadeh, R. Neueder, W. Kunz, Vapor Pressures, Osmotic and Activity Coefficients of Electrolytes in Protic Solvents at Different Temperatures. 2. Lithium Bromide in Ethanol, Journal of Solution Chemistry. 33 (2004) 1429–1446, https://doi.org/10.1007/s10953-004-1057-9.

[19] Y. Lin, A. ten Kate, M. Moojier, J. Deldago, P.L. Fosbal, K. Thomsen, Comparison of Activity Coefficient Models for Electrolyte Systems, AIChE Journal. 56 (2009) 1334–1351, https://doi.org/10.1002/aic.12040.

[20] ENRTL-RK, (2023). https://knowledgecenter.aspentech.com.

[21] T. Chou, A. Tanioka, W. Model, Predicting the Effect of Dissolved Salt on the Vapor-Liquid Equilibria for Alcohol-Water-Salt Systems, 77 (1999) 329–334.

[22] L.A. Cisternas, E.J. Lam, An analytic correlation for the vapour pressure of aqueous and non-aqueous solutions of single and mixed electrolytes. Part II. Application and extension, Fluid Phase Equilibria. 62 (1991) 11–27, https://doi.org/10.1016/0378-3812(91)87002-Q.

[23] P.D. Ghuge, N.A. Mail, S.S. Joshi, Fluid Phase Equilibria Effect of CaCl 2 and ZnCl 2 salts on isobaric vapor-liquid equilibrium in separation of the azeotropic mixture of ethanol + water, Fluid Phase Equilibria. 537 (2021) 113000, https://doi.org/10.1016/j.fluid.2021.113000.

[24] Y. Yao, S. Liu, Basic Equations for Properties of Common Liquid Desiccants, in: Ultrasonic Technology for Desiccant Regeneration, Wiley, 2014, pp. 293–306.

[25] D.-J. Seo, A. Takenaka, H. Fujita, K. Mochidzuki, A. Sakoda, Practical considerations for a simple ethanol concentration from a fermentation broth via a single adsorptive process using molecular-sieving carbon, Renewable Energy. 118 (2018) 257–264, https://doi.org/10.1016/j.renene.2017.11.019.

[26] W. Knoche, Chemical Reactions of CO2 in Water, in: Biophysics and Physiology of Carbon Dioxide, Proceedings in Life Sciences, 1980: pp. 3–11.

[27] C.R. Silva, M.N. Esperança, A.J.G. Cruz, L.F. Moura, A.C. Badino, Stripping of ethanol with CO2 in bubble columns: Effects of operating conditions and modeling, Chemical Engineering Research and Design. 102 (2015) 150–160, https://doi.org/10.1016/j.cherd.2015.06.022.

[28] J. Daniell, M. Köpke, S.D. Simpson, Commercial Biomass Syngas Fermentation, Energies. 5 (2012) 5372–5417, https://doi.org/10.3390/en5125372.

[29] F. Mandani, H. Ettouney, H. El-Dessouky, LiBr-H2O absorption heat pump for single-effect evaporation desalination process, Desalination. 128 (2000) 161–176, https://doi.org/10.1016/S0011-9164(00)00031-X.

[30] H. Shabgard, M.J. Allen, N. Sharifi, S.P. Benn, A. Faghri, T.L. Bergman, Heat pipe heat exchangers and heat sinks: Opportunities, challenges, applications, analysis, and state of the art, International Journal of Heat and Mass Transfer. 89 (2015) 138–158, https://doi.org/10.1016/j.ijheatmasstransfer.2015.05.020.

[31] Y.M. Chen, C.Y. Sun, Experimental study on the heat and mass transfer of a combined absorber-evaporator exchanger, International Journal of Heat and Mass Transfer. 40 (1997) 961–971, https://doi.org/10.1016/0017-9310(96)00155-X.

[32] Á. Fernández-Naveira, H.N. Abubackar, M.C. Veiga, C. Kennes, Carbon monoxide bioconversion to butanol-ethanol by Clostridium carboxidivorans: kinetics and toxicity of alcohols, Applied Microbiology and Biotechnology. 100 (2016) 4231–4240, https://doi.org/10.1007/s00253-016-7389-8.

[33] Structured packings, Sulzer. https://www.sulzer.com/en/products/separation-technology/structured-packings.

[34] R. Agrawal, Multieffect Distillation for Thermally Coupled Configurations, AIChE Journal. 46 (2000) 2211–2224, https://doi.org/10.1002/aic.690461113.

[35] Horizontal split centrifugal compressors, MAN Energy Solutions. https://www.man-es.com/oil-gas/products/compressors/centrifugal.

[36] A.A. Kiss, R.M. Ignat, S. Bildea, Optimal Extractive Distillation Process for Bioethanol Dehydration, Computer Aided, Process Engineering (2014).

[37] A. Singh, G.P. Rangaiah, Review of Technological Advances in Bioethanol Recovery and Dehydration, Industrial and Engineering Chemistry Research. 56 (2017) 5147–5163, https://doi.org/10.1021/acs.iecr.7b00273.

[38] A.A. Kiss, R.M. Ignat, Optimal Economic Design of an Extractive Distillation Process for Bioethanol Dehydration, Energy, Technology. 1 (2013) 166–170, https://doi.org/10.1002/ente.201200053.

[39] E. Volker, How to design and optimise sieve trays, WelChem. (2020).

[40] A.A. Kiss, C.A. Infante Ferreira, Mechanically Driven Heat Pumps, in: Heat Pumps in Chemical Process Industry, CRC Press, Boca Raton, 2016: pp. 189–251.

[41] M. Tatlier, G. Munz, S.K. Henninger, Microporous and Mesoporous Materials Relation of water adsorption capacities of zeolites with their structural properties, Microporous and Mesoporous Materials. 264 (2018) 70–75, https://doi.org/10.1016/j.micromeso.2017.12.031.

[42] A.A. Kiss, D.-J.-P.-C. Suszwalak, Enhanced bioethanol dehydration by extractive and azeotropic distillation in dividing-wall columns, Separation and Purification Technology. 86 (2012) 70–78, https://doi.org/10.1016/j.seppur.2011.10.022.

[43] A. Meirelles, S. Weiss, H. Herfurth, S. Verfahrenstechnik, T. Hochschule, C. Schorlemmer, Ethanol Dehydration by Extractive Distillation (1992) 181–188.

[44] M. Errico, B. Rong, Synthesis of new separation processes for bioethanol production by extractive distillation, Separation and Purification Technology. 96 (2012) 58–67, https://doi.org/10.1016/j.seppur.2012.05.022.

[45] T. Janković, A.J.J. Straathof, A.A. Kiss, Advanced downstream processing of bioethanol from syngas fermentation, Separation and Purification Technology. 322 (2023) 124320, https://doi.org/10.1016/j.seppur.2023.124320.

[46] SPRSUN, What Is a Good COP for an Air to Water Heat Pump?. (2021).

[47] BP, Approximate Conversion Factors, Statistical Review of World Energy. (2021).

[48] D. Humbird, R. Davis, L. Tao, C. Kinchin, D. Hsu, A. Aden, P. Schoen, J. Lukas, B. Olthof, M. Wordey, D. Sexton, D. Dudgeon, Process Design and Economics for Biochemical Conversion of Lignocellulosic Biomass to Ethanol, 2011.

[49] A.A. Kiss, Design, control and economics of distillation, in: Advanced Distillation Technologies: Design, Control and Application, Wiley, 2013: pp. 37–66.

[50] J. Mantingh, A.A. Kiss, Enhanced process for energy efficient extraction of 1, 3-butadiene from a crude C4 cut, Separation and Purification Technology. 267 (2021) 118656, https://doi.org/10.1016/j.seppur.2021.118656.

[51] Marpa, Roots vacuum pumps. https://marpavacuum.com/en/roots-vacuum-pumps.

[52] J. Schwarz, B. Beloff, E. Beaver, Use Sustainability Metrics to Guide Decision-Making, Chemical Engineering Progress. 98 (2002) 58–63.

[53] Directive 2012/27/EU of the European Parliament and of the Council of 25 October 2012 on energy efficiency, amending Directives 2009/125/EC and 2010/30/EU and repealing Directives 2004/8/EC and 2006/32/EC, Official Journal of European Union. (2012).

[54] I. Patrascu, C.S. Bildea, A.A. Kiss, Novel eco-efficient process for dimethyl carbonate production by indirect alcoholysis of urea, Chemical Engineering Research and Design. 160 (2020) 486–498, https://doi.org/10.1016/j.cherd.2020.06.020.

[55] N.P. Lieberman, E.T. Lieberman, Steam Generation, in: A Working Guide to Process Equipment, McGrawHill, 2022: pp. 261–276.

[56] A.A. Kiss, D.J.C. Suszwalak, Innovative dimethyl ether synthesis in a reactive dividing-wall column, Computers and Chemical Engineering. 38 (2012) 74–81, https://doi.org/10.1016/j.compchemeng.2011.11.012.